

# RYDBERG ATOMS: HIGH-RESOLUTION SPECTROSCOPY AND RADIATION INTERACTION— RYDBERG MOLECULES

*J. A. C. GALLAS,<sup>1</sup> G. LEUCHS,<sup>2</sup> H. WALTHER,<sup>1,2</sup> and  
H. FIGGER<sup>1</sup>*

<sup>1</sup>*Max-Planck-Institut für Quantenoptik and*

<sup>2</sup>*Sektion Physik der Universität München  
Garching, Federal Republic of Germany*

I. Introduction . . . . .	414
II. General Properties of Rydberg Atoms . . . . .	416
III. Excitation and Detection of Rydberg States . . . . .	419
IV. Methods of High-Resolution Spectroscopy of Rydberg States . . . . .	421
A. Atomic Beam . . . . .	421
B. Two-Photon Absorption . . . . .	423
C. Double Resonance . . . . .	423
D. Quantum Beat and Level Crossing Techniques . . . . .	425
V. Results of High-Resolution Spectroscopy of Rydberg States . . . . .	427
A. Alkaline Atoms—Fine Structure . . . . .	427
B. Alkaline Atoms—Hyperfine Structure . . . . .	431
C. Alkaline Earth Atoms . . . . .	433
VI. Interaction of Rydberg Atoms with Blackbody Radiation . . . . .	435
VII. Radiation Interaction of Rydberg Atoms—A Test System for Simple Quantum Electrodynamical Effects . . . . .	440
A. Single Atom in Resonant Cavity—Modification of Spontaneous Emission Rates . . . . .	441
B. Single Atom in Resonant Cavity—Disappearance and Revival of Optical Nutation . . . . .	446
C. <i>N</i> Atoms in Resonant Cavity—Collective Behavior . . . . .	446
D. <i>N</i> Atoms in Resonant Cavity—Collective Absorption of Blackbody Photons . . . . .	449
VIII. Rydberg States of Molecules . . . . .	450
A. Rydberg States of Diatomic Molecules . . . . .	452
B. Rydberg States of Large Molecules . . . . .	456
IX. Rydberg Molecules . . . . .	457
References . . . . .	460

## I. Introduction

This article is one of two in the present volume which discuss recent research on Rydberg atoms and molecules. It is concerned with general properties of Rydberg atoms, methods of production and detection, and spectroscopic techniques and results, mainly for alkali and alkali-earth metals, and for the interaction of such atoms with blackbody radiation. The spectroscopy on Rydberg molecules is discussed in the last two sections. The contribution by Haroche and Raimond (H.R.) is devoted to one branch of Rydberg atom research, the radiative properties of such atoms in resonant cavities.

When a valence electron of an atom is excited in an orbit with high principal quantum number and therefore far from the ionic core, the energy levels of the atom can simply be described by the Rydberg formula. This is the reason why atoms in these highly excited states are often called Rydberg atoms. Similarly the highly excited valence electron of a molecule will sense the molecular ion essentially as a positive point charge. Consequently its energy levels can be described by a Rydberg formula also. Differences between Rydberg states of atoms and molecules arise from rotational vibrational excitations of the molecular ion. This leads to drastic effects when the frequency of the orbiting electron becomes comparable to the rotational vibrational frequencies. As a result one finds a breakdown of the Born–Oppenheimer approximation and observes autoionization if part of the rotational vibrational energy is transferred to the Rydberg electron. For a certain class of molecules even low-lying excited states show typical properties of Rydberg states. In the literature they are therefore referred to as Rydberg molecules. These molecular aspects are addressed in Sections VIII and IX, whereas the following discussion, as well as Sections II–VII, concentrate on atomic Rydberg states.

The energy changes among highly excited states of atoms are small compared to the large changes between the lower levels. Since smooth changes are characteristic of classical systems (in which energy changes are continuous), Rydberg atoms can be expected to show classical properties. In particular, according to Bohr's correspondence principle, the frequency of electromagnetic radiation emitted for transitions between neighboring states approaches the frequency at which the electron rotates around the ionic core. This suggests that many properties of these atoms can be understood in simple classical terms. Nevertheless, some very surprising properties of Rydberg atoms have recently been found, which has led to a steady increase in the number of experiments being performed on these atoms. The interest in Rydberg states is manifold:

(1) The outer electron is a very good probe for the interatomic potential; quantum defects due to the penetration and polarization of the electron core are therefore being investigated, as well as fine- and hyperfine-structure splittings.

(2) Radiation effects are different from those for atoms in low-lying states owing to the large matrix elements for transitions to neighboring levels; radiation-induced effects therefore overcome spontaneous emission. The Rydberg atoms in high  $n$  states become sensitive to blackbody radiation, and maser emission with only a small absolute number of radiators can also be observed. Observation and study of these effects allows testing of fundamental theories on light-matter interaction, which is not possible with ordinary atoms.

(3) Collisional interaction becomes very important owing to the size of the atoms; their influence shows strong dependence on the main quantum numbers. It is thus found, for example, for the collisional angular momentum mixing in the low  $n$  region that the cross section increases in proportion to the geometric size of the atoms, i.e.,  $n^4$ . As the size of the Rydberg orbit increases further, the electron distribution becomes very diffuse and the cross section goes through a maximum and decreases. This is the case for collisions with neutral particles, with which the Rydberg electron interacts only weakly via the induced polarization. For charged particles which interact with the Rydberg electron via the long-ranging Coulomb interaction, the cross section keeps increasing.

(4) The binding energy of the electron to the ionic core is very small; the Rydberg atom is therefore strongly influenced by external electric and magnetic fields.

This article is mainly concerned with high-resolution spectroscopy and interaction of Rydberg atoms with radiation. The other fields, e.g., collisions and interaction in external electric and magnetic fields, were covered some time ago and will therefore not be included here (see Edelman and Gallagher, 1978; Stebbings, 1979; Feneuille and Jacquinet, 1981; Kleppner, 1982; Kleppner *et al.*, 1983).

The first observation of Rydberg states dates back to the end of the last century when Livering and Dewar (1879) described the observations of long series in alkali spectra. Ten years later Rydberg (1889) proposed the famous formula  $E_n = -R/(n - \delta)^2$ , where the quantum defect  $\delta$  is approximately constant in a given series, so that the effective quantum number  $n^* = n - \delta$  increases by integers. At the beginning of this century Bevan (1912) observed 31 members of the principal series of the cesium spectrum, while Wood (1916) photographed 57 members in sodium. Observation in emission was

impossible since the electrons in highly excited states are so weakly bound that the atoms are ionized by collisions before they can radiate.

Emission from isolated Rydberg atoms was first observed in interstellar space: many emission lines corresponding to transitions between neighboring levels with high quantum numbers are detected in radio astronomy. In space the Rydberg atoms are created by the recombination of electrons and protons to hydrogen; the atoms radiate as they cascade to lower and lower states. The first line discovered in radio astronomy is at 5.4 GHz and corresponds to a transition between the states  $n = 110$  and  $n = 109$  of hydrogen. It was observed in the Orion nebula (Kardashev, 1960; Höglund and Mezger, 1965).

The population of highly excited states under collision-free conditions became possible with the advent of tunable laser sources. Individual states can now be populated and their properties studied in detail in the laboratory.

## II. General Properties of Rydberg Atoms

The properties of the Rydberg atoms are very much hydrogen-like. Their energy is given by the Rydberg formula (Table I).  $R$  is the Rydberg constant and  $\delta_l$  the phenomenological quantum defect of the states of angular momentum  $l$ . For states of low  $l$ , where the orbits of the classical Bohr-Sommerfeld theory are ellipses of high eccentricity, the penetration and polarization of the electron core by the valence electron lead to large quantum defects and strong departures from the hydrogenic behavior. As  $l$  increases, the orbits become more circular and the atom becomes more hydrogenic:  $\delta_l$  changes with  $l^{-5}$ . In Table I the scaling laws for further properties of Rydberg atoms are compiled: the radius of the charge distribution of the

TABLE I

SCALING LAWS FOR PROPERTIES OF RYDBERG ATOMS<sup>a</sup>

Energy:	$E_{nl} = R/(n - \delta_l)^2 = R/n^{*2}$ $n^*$ effective quantum number, $\delta_l$ quantum defect
Radius:	$\langle r \rangle \sim n^{*2}$
Lifetimes:	$\tau \sim n^{*3}$ (low angular momentum states) $\tau \sim n^{*5}$ (high angular momentum states)
Fine-structure interval:	$\Delta E \sim n^{*-3}$

<sup>a</sup> For details see text.

valence electron scales as  $n^{*2}$ , and for  $n^* = 50$  the linear dimension of the atom is already comparable with the wavelength of light in the visible region and competes with the size of the large biomolecules.

The electric polarizability for the quadratic Stark effect increases as  $n^{*7}$ , and the diamagnetic interaction as  $n^{*4}$ . This allows one to perform experiments at field strengths high enough to make the interaction energy in the external electric or magnetic field comparable with or larger than the Coulomb energy of the atom. For practical reasons the corresponding field strengths for ground state atoms cannot be reached in the laboratory. The study of highly excited atoms in external electric and magnetic fields is therefore interesting in itself. For reviews see Feneuille and Jaquinot (1981), Kleppner (1982), Kleppner *et al.* (1983), and Delande and Gay (1983). The sensitivity of Rydberg atoms to external electric fields also means that the atoms readily ionize in rather weak fields. This opens the possibility of very effective detection, as will be discussed later.

The large Rydberg atom orbitals are characterized by natural lifetimes much longer than those of less excited atoms. In the case of hydrogen Rydberg states, the dependence of the lifetime on  $n$  can be obtained by fully quantum mechanical radiation rate calculations involving hydrogenic coulombic wave functions. For Rydberg states of other species the lifetimes (and the other radiative parameters) do not scale exactly as a power of  $n$  but rather as a power of  $n^*$ . The  $n^*$  scaling law can be determined by using calculations of the Bates and Damgaard (1949) type. The lifetimes scale either as  $n^{*3}$  (when  $l$  is small) or as  $n^{*5}$  (when  $l \cong n$ ).

In the following we will give a simple explanation of this scaling law. (In this discussion we do not discriminate between  $n$  and  $n^*$ .) The rate of spontaneous emission of radiation for a transition from a state  $n$  to  $n'$  is given by the Einstein  $A$  coefficient:

$$A_{n \rightarrow n'} = 16\pi^3 \nu^3 e^2 \langle r_{nn'} \rangle^2 / 3\epsilon_0 \hbar c^3 \quad (1)$$

where  $\nu$  is the transition frequency and  $\langle r_{nn'} \rangle$  the matrix element of the electric dipole operator between the initial  $n$  and the final state  $n'$ . For the case  $n' \ll n$  one has a small  $\langle r_{nn'} \rangle$  owing to the small radial overlap of the wave functions for  $n$  and  $n'$  and, as will be shown below,  $A_{n \rightarrow n'} \sim n^{-3}$ . If  $n'$  is close to  $n$ , the energy difference  $E_n - E_{n'} \sim n^{-3}$  and  $\langle r_{nn'} \rangle^2 \sim n^4$ , and so  $A_{n \rightarrow n'}$  becomes proportional to  $n^{-5}$ . The magnitude of the Einstein coefficient  $A_{n \rightarrow n'}$  still depends on the angular momentum  $l$ . This can be understood by simple classical arguments: For low angular momentum states (core penetration) the lifetime  $\tau$  can be deduced from the third Kepler law. Accordingly, the electron orbiting period  $T$  is given by  $T \cong (n^2 a_0)^{3/2} \cong n^3$  (in the classical picture  $T$  must be proportional to  $\tau$  since transition to a lower orbit is always more probable when the electron approaches the core and under-

goes maximum acceleration). For the case of high angular momentum orbitals, in the classical picture, the electron radiates continuously and lowers its radius. The acceleration of the electron is inversely proportional to the square of the radius of the orbit, and so the power of the emitted radiation scales as  $n^{-8}$ . The distance between neighboring Rydberg levels changes as  $n^{-3}$ , giving a characteristic time requirement of  $n^{-3}/n^{-8} = n^5$  for each step, which corresponds to the lifetime for states with large  $l$ . The square of the matrix element  $\langle r_{nn'} \rangle$  ( $n \cong n'$ ) scales as  $n^4$ , showing a rather high transition probability for induced transitions. Rydberg atoms therefore strongly absorb microwave or far-infrared radiation. As a consequence, blackbody radiation may cause strong mixing of the states. This is especially the case for states with high angular momenta since the spontaneous lifetimes for these are much longer and the induced transitions can therefore be saturated much more easily than for the lower  $l$  states.

We now wish to discuss also the scaling laws relating to blackbody-induced effects. A much more detailed discussion is presented later in Section VI.

The induced transition rate due to blackbody radiation is proportional to  $\langle r_{nn'} \rangle^2 S_\nu$ , where  $S_\nu$  is the energy flux of the blackbody radiation per unit band width and unit surface area. At low frequencies (Rayleigh–Jeans limit)  $S_\nu$  increases as  $\nu^2$ . As the distance between the Rydberg states scales as  $n^{-3}$  (here again we conduct the discussion with  $n$  instead of  $n^*$ ), it is therefore found that  $S_\nu$  is proportional to  $n^{-6}$ . Since  $\langle r_{nn'} \rangle^2 \sim n^4$ , it follows that the induced transition rate behaves as  $n^{-2}$ . Important in experiments is the ratio between the induced transition rate and the spontaneous rate, which changes as  $n^{-3}$  for low  $l$  and as  $n^{-5}$  for high  $l$ . This means that for a given atom and a given temperature there exists an  $n$  above which the blackbody-induced rate overcomes the spontaneous rate.

The sensitivity of Rydberg atoms to blackbody radiation can also be explained in the following terms. The blackbody radiation energy density can be expressed in terms of the number of photons per mode  $\bar{n}$ . For the Rayleigh–Jeans limit this gives  $\bar{n} = kT/h\nu$ . At 300 K it follows that  $kT/h \cong 6 \times 10^{12}$  Hz; this means that for frequencies larger than  $kT/h$ , where  $\bar{n} \ll 1$ , no significant blackbody influence can be observed. However, for a Rydberg state with a transition frequency to a neighboring state at  $10^{11}$  Hz, where  $\bar{n} = 60$ , the blackbody-induced transition rates can be orders of magnitude larger than the spontaneous rates.

The interaction of blackbody radiation with atoms is, in principle, nothing new since incandescent lamps are used for absorption spectroscopy in the visible spectrum. However, the fact that room-temperature radiation is important can only be observed with Rydberg atoms. In addition to population changes induced by the blackbody radiation, energy shifts of the atomic levels also occur. Their magnitudes depend on the match of the atomic

frequencies with the most probable blackbody frequencies and the strength of the coupling of the Rydberg atom to the blackbody radiation (these effects will also be discussed in more detail in Section VI).

### III. Excitation and Detection of Rydberg States

In absorption spectroscopy with classical light sources only those Rydberg states could be investigated which can be optically excited directly from the ground state. For spectra of atoms with one valence electron this means that only the  $^2P$  series can be studied (Moore, 1971). The alternative method of populating Rydberg states in an electric discharge and observing the spectrally resolved fluorescence is not practical: at the required particle densities collisional deactivation is much more probable than radiative decay, since it is a result of the large collisional cross sections of Rydberg states and of the long lifetimes. However, in atomic beam experiments where one can reach collision-free conditions it is possible to use electron bombardment or charge exchange collisions to populate and study Rydberg states (e.g., Bayfield and Koch, 1974). Some experiments have exploited this effect. One drawback of this excitation process, however, is that it is not state selective. It was due to these limitations of the techniques of classical spectroscopy that after the invention of frequency-tunable lasers, little more than a decade ago, there was a renaissance of the spectroscopy of highly excited atomic states. The use of lasers to populate high-lying atomic levels in one, two, or three excitation steps considerably increased the number of atomic states accessible to experiments. In particular, states with the same parity as the ground state could be reached. For atoms with large ionization potentials it can be advantageous to combine the collisional excitation of metastable states and subsequent laser excitation to Rydberg states (Stebbins *et al.*, 1975; Barbier and Champeau, 1980; Rempe, 1981).

For high-resolution spectroscopy of Rydberg atoms a low atom density is required in order to avoid collisional broadening or a collisional shift. This excludes absorption measurement from the outset since larger densities are required there. The alternative method of observing the fluorescence, however, is not suitable either for high-lying states ( $n \geq 15$ ), since the  $n^3$  dependence of the radiative lifetime implies a corresponding decrease of the fluorescence intensity. Most experiments therefore exploit collisional, photo- or field ionization to detect Rydberg atoms.

Collisional ionization is the mechanism used in the thermionic diode (Popescu *et al.*, 1966), which was later refined by Harvey and Stoicheff

(1977) and also by, for example, Beigang *et al.* (1983). The sensitivity of this device, if operated in the space-charge-limited regime, approaches that achieved by ion detection with multipliers.

Rydberg atoms can also be detected by photoionization where either the ions or the electrons are recorded by means of a multiplier. Detecting the photoelectrons has the advantage that their angular distribution can be measured, thus providing additional information on properties of the Rydberg states which is not accessible in total cross-section measurements. When the use of photoionization is considered, it is important to know the cross section, which determines the efficiency of the process. If the wavelength of the ionizing laser is always readjusted so that the threshold for ionization is just reached, the photoionization cross section increases linearly with  $n$  (Aymar *et al.*, 1976). If, however, a fixed laser wavelength is used, the cross section decreases as  $n^{-3}$  (Kramers, 1923; Menzel and Pekeris, 1935; Burgess, 1964). When photoionizing, for example high-lying  $d$  states of sodium with a Nd:YAG laser, it is difficult to observe signals from  $n > 40$  (Leuchs, 1983).

The most widely used method of detection of Rydberg atoms is the ionization in an external electric field. Field ionization was first observed in hydrogen, where about  $10^6$  V/cm has to be applied to ionize the  $n = 4$  states (Rausch von Traubenberg *et al.*, 1930). In the range of  $n = 30$  an electric field of only 300 V/cm is enough to reach the onset of field ionization. The superposition of the atomic Coulomb potential and the linear slope potential of the externally applied field result in a potential structure having a saddle point. The simplest approach to field ionization is to say that states above the saddle point fully ionize and states below are stable. For a state with principal quantum number  $n$  there exists a critical field defined by the onset of field ionization. Using the simple potential picture, one obtains (Feneuille and Jaquinot, 1981)

$$E_{\text{crit}} \propto 1/n^4 \quad (2)$$

As long as spectroscopic information about the unperturbed Rydberg atom is wanted, the excitation of the Rydberg state and field ionization have to be separated in time. If an electric field ramp is applied, after a time lag with respect to pulsed laser excitation, Rydberg atoms in different  $n$  states will ionize at different electric fields, i.e., at different times, and can thus be discriminated.

For electric fields high enough to ionize a Rydberg atom, the force on the valence electron due to the external electric field is larger than the Coulomb force and is therefore not at all a small perturbation. If the electric field is increased to such a high value, the evolution of the atom is rather complicated. This can be seen from experimental Stark effect studies, which display

a large number of magnetic substates and avoided crossings between them (Littman *et al.*, 1978). A detailed discussion of the electric field effects is beyond the scope of this article (see Kleppner *et al.*, 1983). It is, however, important to note that, for example, the electric field at which a given Rydberg state ionizes depends critically on the rise time of the electric field pulse (Jeys *et al.*, 1980; Vialle and Duong, 1979; Neijzen and Dönszelman, 1982). This corresponds to either diabatic or adiabatic passage through the various avoided crossings (Rubbmark *et al.*, 1981).

In summary, field ionization allows discrimination of different Rydberg states even of different fine structure levels of the same  $nl$  state (Gallagher *et al.*, 1978) and is highly efficient.

#### IV. Methods of High-Resolution Spectroscopy of Rydberg States

There is a great deal of experimental data on Rydberg levels measured with moderate spectral resolution, these being often analyzed by means of single or multichannel quantum theory (Feneuille and Jaquinot, 1981). These experiments are not discussed here, however. Attention is focused on spectroscopic techniques which allow Doppler-free resolution of narrow spectral structures of Rydberg levels. Among these are of course the techniques of classical high-resolution spectroscopy, namely the atomic beam, double resonance, level crossing, and quantum beat technique. Of the new nonlinear techniques of laser spectroscopy only Doppler-free two-photon absorption has been used for Rydberg states. Table II shows what combinations of spectroscopic techniques and detection mechanisms have already been realized experimentally. It is obvious that for states with principal quantum numbers  $n > 20$  detection by field ionization takes the role of fluorescence detection at low  $n$  values. Detection by collisional ionization has mainly been used in connection with the thermionic diode. Photoionization can be used as a detection mechanism for any technique listed in Table II. For low-lying states this has been demonstrated in particular for the level crossing (Luk *et al.*, 1981) and quantum beat (Leuchs *et al.*, 1979; Hellmuth *et al.*, 1981) methods.

##### A. ATOMIC BEAM

Many of the experiments listed in Table II were performed with the use of thermal atomic beams to achieve collision-free conditions. Here, however, we refer to the atomic beam technique only when the well-directed motion of

TABLE II

SURVEY OF EXPERIMENTAL TECHNIQUES USED TO PERFORM DOPPLER-FREE MEASUREMENTS OF RYDBERG STATES<sup>a</sup>

Excitation	Doppler-free method	Detection			
		Fluorescence	Collisional ionization	Field ionization	Photoionization
Narrow-band excitation	Atomic beam	Frederiksson <i>et al.</i> (1980)	—	Meschede and Walther (1983) Lieberman and Pinard (1979) Barbier and Champeau (1980)	Solarz <i>et al.</i> (1976)
	Two-photon absorption	Kato and Stoicheff (1976) Harper and Levenson (1976)	Niemax and Pendrill (1980) Harvey and Stoicheff (1977) Stoicheff and Weinberger (1979) Beigang <i>et al.</i> (1981)	Lee <i>et al.</i> <sup>b</sup> (1979) Meschede and Walther (1983)	
Broad-band excitation (pulsed)	Double resonance (HF)	Farley <i>et al.</i> (1979) Gallagher <i>et al.</i> (1976)	—	Gallagher <i>et al.</i> (1977) Fabre <i>et al.</i> (1977) Meschede and Walther (1983)	—
	Level crossing	Frederiksson and Svanberg (1976)	—	—	Luk <i>et al.</i> (1981) <sup>c</sup>
	Quantum beats	Fabre <i>et al.</i> (1975)	—	Jeys <i>et al.</i> (1980) Leuchs and Walther (1977; 1979)	Leuchs <i>et al.</i> (1979) <sup>c</sup> Hellmuth <i>et al.</i> (1981) <sup>c</sup>

<sup>a</sup> For a complete survey on the measurements performed, see Section V.<sup>b</sup> Method of separated fields (Ramsey fringes) used to reduce transit time broadening.<sup>c</sup> Demonstrated for low-lying excited states.

atoms in a collimated beam is used to reduce the Doppler broadening. This is achieved by crossing the atomic beam at right angles with a narrow-band laser beam. At a collimation ratio of 1 : 1000 the residual Doppler effect at optical transition frequencies is of the order of a few megahertz, which is about the line width of commercially available dye lasers. The detection of the atoms is geometrically separated from the region where the laser excitation takes place and is performed by field ionization.

## B. TWO-PHOTON ABSORPTION

The technique of suppressing the first-order Doppler effect by absorbing two photons, first proposed by Vasilenko *et al.*, (1970), is also successfully applied to the spectroscopy of Rydberg states. In this method the atoms are excited by two laser beams traveling in opposite directions. An atom moving in the cell with a velocity component  $v_z$  sees the frequencies of the two laser beams Doppler-shifted by the amounts  $(1 - v_z/c)$  and  $(1 + v_z/c)$ , respectively. If the atom performs the two-photon transition by absorbing one photon from each of the two beams, the influence of the Doppler shift is canceled. The essential point is that the Doppler width is compensated for all atoms: the whole ensemble, which is illuminated by the laser beams, contributes to the signal, and so experiments can be performed in a cell. The combination of Doppler-free two-photon absorption and collisional ionization in a thermionic diode has proved to be especially successful. One of the reasons is that the thermionic diode operated in the space-charge-limited regime is a highly efficient device easy to use. The spectral resolution achieved is often limited by the finite laser line width typically around 1 MHz. When lasers with a much smaller line width are used the resolution is mostly limited by the finite transit time of the atoms through the laser beam. One way to overcome this limitation is to increase the laser beam diameter, which of course lowers the laser intensity. An alternative approach is Ramsey's method of separated fields (Baklanov *et al.*, 1976) which was demonstrated for Rydberg atoms by Lee *et al.* (1979). The resolution obtained was 10 KHz. At this level of resolution one also has to consider the second-order Doppler effect, which is not compensated for by these methods discussed so far.

## C. DOUBLE RESONANCE

For the two methods discussed so far frequency-tunable lasers with a narrow line width have to be used. For the techniques described in the

remainder of this section this is not necessary. In the double-resonance technique, pioneered by Brossel *et al.* (1950), an excited state of an atom is populated by optical radiation. This excited state will subsequently decay via spontaneous emission of radiation, having well-defined polarization and angular distribution. Microwave or radio frequency radiation inducing transitions to neighboring excited states will change the spatial distribution of the fluorescence or the polarization, allowing sensitive detection of the microwave resonances. For Rydberg states, where the observation of the fluorescence is difficult, it has been demonstrated that different states often have characteristically different field ionization behavior. Consequently, microwave resonances between Rydberg states can be very efficiently detected by using field ionization (Fig. 1). Let us assume that the atoms are optically excited in the lower level by pulsed laser radiation. Then they are exposed to microwave radiation. At a later time field ionization is performed by an electric field ramp. When the field reaches the ionization threshold ( $F_2$ ) of the upper level a gated integrator samples either the electron or ion current. The signal obtained is therefore proportional to the population of the upper level (Fig. 1). The resonance can be measured by varying the microwave frequency. Here, an important factor is the large cross sections

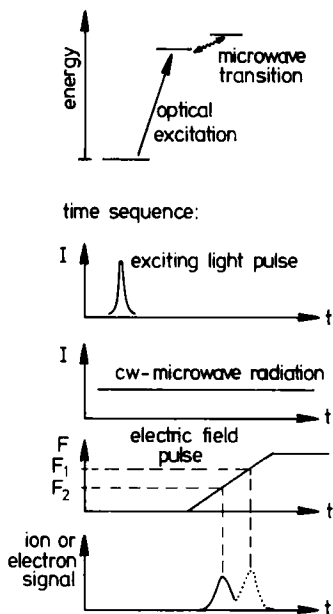


FIG. 1. Principle of the optical microwave double-resonance method applied to Rydberg atoms. The field ionization signal (solid line, lower part of the figure) at the field  $F_2$  is only observed when the microwave radiation is in resonance with the transition.

for absorption of microwave photons between neighboring Rydberg state, discussed in detail in Sections III and VI. In general, the line width in an optical double-resonance experiment is Doppler broadened, but it turns out to be small since the Doppler width is proportional to the microwave transition frequency.

#### D. QUANTUM BEAT AND LEVEL CROSSING TECHNIQUES

In a quantum beat experiment atoms are excited into a coherent superposition of neighboring states by using a short light pulse the duration  $\Delta t$  of which meets the condition  $(\Delta t)^{-1} > \Delta E/h$ , where  $\Delta E$  is the energy distance between the two excited states. The subsequent evolution of the atoms is observed time resolved via the fluorescence or by probing the atoms with an additional light pulse after a variable delay time. The signal as a function of time (fluorescence) or of the delay time (probing pulse) exhibits a periodic variation, the frequency of which gives the energy separation of the states under consideration.

The reason for this oscillating behavior in time is that the phases of the wave functions of the excited states evolve differently in time and their changes are related to the frequency separation of the states. In the density matrix formalism the signal beats result from the time variation of the non-zero off-diagonal elements of the density matrix.

In order to observe the quantum beats, the detection process has to be sensitive to the off-diagonal elements of the density matrix. This means that the detection process should not discriminate between the states excited by the light pulse or, in other words, the excitation and detection channels via the neighboring states should be indistinguishable by analogy with Young's double-slit experiment. Otherwise quantum beats will not be observed. In the case of higher lying Rydberg states it is difficult to observe quantum beats in fluorescence or in absorption to higher bound states. However, when the second step is a bound-free transition into the continuum, quantum beats are easier to observe. The quantum interferences are also observable when field ionization is used for detection (see Fig. 2). The first experiments of this kind were performed by Leuchs and Walther (1977 and 1979) on the  $n^2D$  fine-structure states of sodium ( $n = 21$  to 30). Later the application of the method was extended to levels up to  $n = 40$  by Jeys *et al.* (1980).

Detection of quantum beats by field ionization is possible since the different magnetic sublevels  $m_l$  ionize at different fields (Rausch von Traubenberg *et al.*, 1930; Gallagher *et al.*, 1977; Jacquinet *et al.*, 1977). With the strength of the ionizing electric field pulse properly adjusted, field ionization allows one to detect the spatial anisotropy of the excited states. The other require-

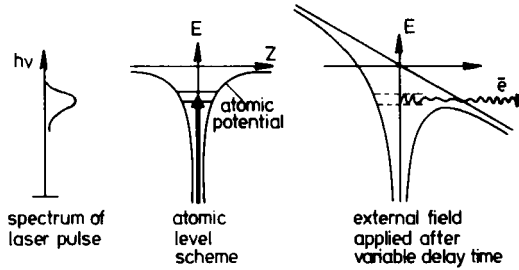


FIG. 2. Scheme for quantum beat experiments using field ionization for detection. The excitation-ionization channels via the excited states have to be indistinguishable as in Young's interference experiment. The quantum interference signals are observed in the total electron current measured as a function of the time delay between the excitation and field ionization.

ment, the indistinguishability of the ionization via the different levels, can be met by using short rise times for the time-delayed field ionization pulse, so that at least one of the adiabatically avoided crossings existing between the different Stark substates is practically crossed diabatically. The dependence of the quantum beat signal on the rise time of the field ionization pulse was nicely demonstrated by Jeys *et al.* (1980). The frequency resolution is determined by the maximum variation of the time delay between the exciting light pulse and the electric field pulse used for ionization. A quantum beat signal obtained by this method is shown in Fig. 3. The maximum time delay in this measurement was 5  $\mu\text{sec}$ .

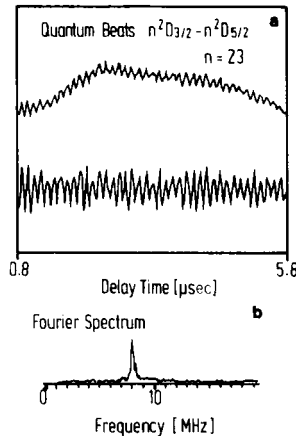


FIG. 3. Quantum beat signal of the fine-structure splitting of the  $23^2D$  state of sodium. The upper trace shows the experimental recording. In the lower trace the slowly varying background which is caused by geometric effects in the electron detection is subtracted. The fine-structure splitting frequency is obtained by a Fourier analysis of the quantum beat signal. For details see Leuchs and Walther (1979).

The level crossing technique is essentially a time-integrated observation of quantum beats. Whenever the quantum beat frequency is too high, the integration will average out the quantum beat oscillations. Only if the beat period is longer than the lifetime of the excited states—or whatever determines the effective integration time—can a net effect be seen in the time-integrated signal. In a level crossing experiment usually a magnetic field is applied, causing Zeeman splitting. The difference in the phase variations of the two Zeeman levels goes through zero whenever two levels cross, giving an extreme value in the time-integrated signal. So far the level crossing technique has been applied to the spectroscopy of Rydberg states only in combination with the detection of the fluorescence.

## V. Results of High-Resolution Spectroscopy of Rydberg States

### A. ALKALINE ATOMS—FINE STRUCTURE

As discussed in Section II an empirical hydrogen-like representation of alkaline atoms in widespread use assumes the valence electron to move around an inner core with electrons in filled shells. In this representation the effective quantum number  $n^*$  is used to account for the incomplete shielding of the nuclear electric field by the core electrons. In the hydrogenic model the fine and hyperfine splitting of the energy levels of the valence electron should show an  $n^{*-3}$  dependence. This simple model does not consider more sophisticated effects which may influence the core, e.g., polarization effects (single core electron excitation) and correlation effects (multiple excitation). This means that deviations from the hydrogenic theory should be expected whenever these effects have an influence. In fact, departures of the experimental fine and hyperfine-structure splittings from the empirical hydrogenic description are normally regarded as indications of these effects. The accurate measurements of such departures can thus serve to uncover details of higher order many-body effects, which are of course also of general interest and may occur for other atoms. In this respect, the methods of high-resolution spectroscopy described above present a sensitive and unique way of achieving this goal.

In recent years many investigations of the fine-structure splitting of the alkaline atoms have been published. Owing to the modern techniques of laser spectroscopy applied in most of the measurements a rather high accuracy has been achieved, so that to date a rather good survey of the effects

involved can be given. Table III summarizes recent papers on the fine structure of alkaline atoms. The observed values of the fine-structure splittings have been fitted to the empirical formula

$$\Delta_{fs} = A/n^{*3} + B/n^{*5} + C/n^{*7} \quad (3)$$

In spite of the success of this empirical treatment, the physical interpretation of the parameters  $A$ ,  $B$ , and  $C$  in Eq. (3) is not well identified. Recently, Pendril (1983) revised the discussion on the validity of omitting even powers of  $n^*$ .

By an analytical evaluation of the  $n$  dependence of the energy eigenvalues of Rydberg states based on the quasi-hydrogenic character of the single-particle eigenfunctions (Chang, 1978; Chang and Larijani, 1980) a somewhat different formula was obtained

$$\Delta_{fs} = N_l(n) (a + b/n^2 + c/n^4 + \dots) \quad (4)$$

$$\text{with } N_l(n) = n^{-3} \prod_{p=0}^l [(n^2 - p^2)/n^2]$$

Equation (4) was used to analyze quantitatively experimental data (Chang and Larijani, 1980). More than one term is especially needed in order to reproduce the low  $n$  behavior. The need for terms involving other than an  $N^{*-3}$  dependence clearly indicates the breakdown of the simple hydrogenic picture. The precise *ab initio* calculation of the fine structures is very difficult and has been undertaken for only a few Rydberg levels of helium (Chang and Poe, 1976) and of more complex alkalis by using high-order perturbation theory (Foley and Sternheimer, 1975; Sternheimer *et al.*, 1976), many-body formalism (Holmgren *et al.*, 1976; Lindgren and Morrison, 1982), pure relativistic central field approach (Luc-Koenig, 1976). The experimental fine-structure intervals, except for Li, are usually larger than the screened hydrogenic values and can even be inverted, as is the case for  $n^2D$  terms of Na, K, and for the  $n^2F$  terms of Rb and Cs. These inversions are particularly interesting because they violate predictions of the simple hydrogenic model, clearly indicating the presence of other effects. In the following the fine structure of the  $n^2D$  terms is discussed in more detail.

In Fig. 4 we compare the fine structure of the Na  $n^2D$  states to that of hydrogen and other alkalis. The references are given in Table III. The values for the  $n^2D$  splittings are multiplied by  $n^{*3}$  and plotted as a function of  $n$ . In the case of a pure  $1/n^{*3}$  dependence horizontal lines are expected. The deviation for Na, K, and Rb is obvious. In the case of Na and K the fine-structure splitting is inverted for all  $n$  states, whereas for Rb only the  $n = 4$  fine structure has a negative sign. The  $1/n^{*3}$  dependence is very well fulfilled

TABLE III

SURVEY OF THE FINE-STRUCTURE MEASUREMENTS PERFORMED ON  
ALKALINE ATOMS

Element	Series	$n$	Reference
Li	P	2	Mingguang <i>et al.</i> (1982)
	D	$7 \leq n \leq 10$	Cooke <i>et al.</i> (1977a)
		4	Fredriksson <i>et al.</i> (1978)
		3	Champeau <i>et al.</i> (1978)
		$4 \leq n \leq 7$	Wangler <i>et al.</i> (1981)
F, G	$7 \leq n \leq 11$	Cooke <i>et al.</i> (1977a)	
Na	P	$16 \leq n \leq 19$	Cooke <i>et al.</i> (1977b)
		$23 \leq n \leq 41$	Fabre <i>et al.</i> (1978); 1980
	D	$9 \leq n \leq 16$	Fabre <i>et al.</i> (1975)
		$4 \leq n \leq 9$	Fredriksson and Svanberg (1976)
		15, 16, 17	Gallagher <i>et al.</i> (1977b)
		$21 \leq n \leq 31$	Leuchs and Walther (1979)
		$32 \leq n \leq 40$	Jeys <i>et al.</i> (1981)
	F	11, 13, 14	Gallagher <i>et al.</i> (1977a)
G, H	$13 \leq n \leq 17$	Gallagher <i>et al.</i> (1976)	
K	S	$9 \leq n \leq 46$	Lorenzen <i>et al.</i> (1981)
	D	$8 \leq n \leq 19$	Harper and Levenson (1976)
		$15 \leq n \leq 20$	Gallagher and Cooke (1978)
		5, 6	Nilsson and Svanberg (1979)
	$7 \leq n \leq 46$	Lorenzen <i>et al.</i> (1981)	
Rb	S	$9 \leq n \leq 116$	Stoicheff and Weinberger (1979)
	P	$28 \leq n \leq 60$	Liberman and Pinard (1979)
	D	$7 \leq n \leq 124$	Stoicheff and Weinberger (1979)
		$4 \leq n \leq 9$	Johansson (1961)
	F	6, 7	Farley and Gupta (1977)
Cs	S	$7 \leq n \leq 11$	Eriksson and Wenáker (1970)
		$12 \leq n \leq 35$	Lorenzen <i>et al.</i> (1980)
		$27 \leq n \leq 44$	Goy <i>et al.</i> (1982)
	P	$7 \leq n \leq 13$	Lorenzen and Niemax (1979)
		$23 \leq n \leq 42$	Goy <i>et al.</i> (1982)
	D	15, 17, 19	Curry <i>et al.</i> (1976)
		$11 \leq n \leq 48$	Lorenzen <i>et al.</i> (1980)
		32	Goy <i>et al.</i> (1982)
	F	$9 \leq n \leq 12$	Eriksson and Wenáker (1970)
		$10 \leq n \leq 17$	Fredriksson <i>et al.</i> (1980)
24, 29, 30		Goy <i>et al.</i> (1982)	

for the higher  $n$  states. In the case of Li the fine-structure values are almost the same as for the hydrogen (deviations are less than 0.5%) and a perfect  $1/n^3$  dependence is found for all  $n$  states (Wangler *et al.*, 1981).

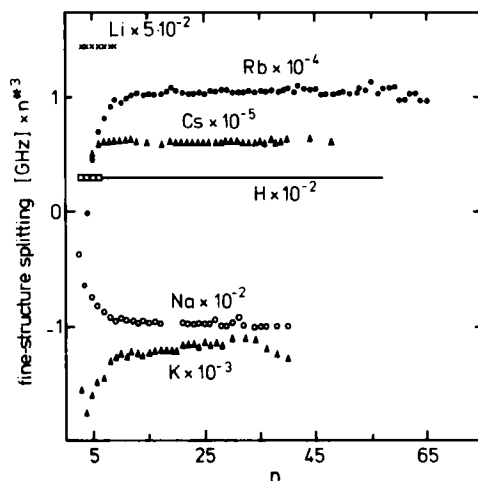


FIG. 4. Fine-structure splitting of the  $n^2D$  states of the alkaline atoms and of hydrogen. The values for the  $n^2D$  splittings are multiplied by  $n^3$ . For references see Table III.

Theoretical calculations for the  $^2D$  fine-structure splitting have only been performed for the Rb  $4^2D$  state and for the Na  $n^2D$  sequence,  $n = 3$  to  $n = 16$ . In the case of the Rb  $4^2D$  state Lee *et al.* (1976) could verify the negative sign of the splitting by calculating the exchange core polarization contribution. However, the value is more than 50% smaller than the experimental result.

Holmgren *et al.* (1976) and Sternheimer *et al.* (1978) performed many-body calculations for the Na  $3^2D$  to  $6^2D$  states including polarization effects to all orders. The negative sign of the splitting is found. However, the values are systematically 25% too small, which the authors attributed to correlation effects not taken into account in their calculations. A better agreement with the experimental values is reached by Luc-Koenig (1976), who calculated the fine-structure splitting of the Na  $^2D$  states for principal quantum numbers from  $n = 3$  to  $n = 16$  with a relativistic central field approximation; the inverted splitting observed in the experiment could be reproduced to within  $\cong 10\%$ , which is a very good agreement. Pyper and Marketos (1981) presented a calculation where the fine-structure inversions in highly excited D and F states are explained as first-order relativistic corrections to the Hartree–Fock energy. Recently refined many-body perturbation calculations also gave a good agreement with the experiment showing that correlation effects are rather small (Lindgren and Martensson, 1982).

To summarize the theoretical results, it seems obvious that the main reason for the inversion of the fine-structure splitting of the  $n^2D$  levels is the polarization of the inner core by the outer electron. An almost quantitative

description is obtained when relativistic effects are included. It is important that for large  $n$  the fine-structure splitting of the alkaline  $^2D$  states scales as  $1/n^{*3}$  no matter whether the splitting is inverted or not.

## B. ALKALINE ATOMS—HYPERFINE STRUCTURE

The hyperfine structure arises basically from the interaction of the magnetic dipole moment of the nucleus with the magnetic moment of the angular motion and the spin of the valence electron. In a simple hydrogen-like picture of the alkaline atoms the magnetic dipole interaction constant can be calculated from the semiempirical formula (Kopfermann, 1958; Belin *et al.*, 1976a,b)

$$a_s = \frac{8}{3} \frac{hcRy}{n^{*3}} \alpha^2 g'_I Z_a^2 Z_i \frac{dn^*}{dn} F_r(j, Z_i) (1 - \delta)(1 - \epsilon) \quad (5)$$

for  $s$  electrons and from

$$a_j = \frac{\mu_0}{4\pi} 2\mu_B^2 g'_I \frac{l(l+1)}{j(j+1)} \langle r^{-3} \rangle F_r(j, Z_i) (1 - \delta)(1 - \epsilon) \quad (6)$$

for non- $s$  electrons. In these formulas  $g'_I$  is the nuclear  $g$  factor referring to Bohr magnetons  $\mu_B$ ,  $Z_a$  is the effective nuclear charge at a large distance from the nucleus (i.e.,  $Z_a = 1$  for a neutral atom;  $Z_i = Z$  for  $s$  electrons, and it is generally set to  $Z_i = Z - 4$  for  $p$  electrons and  $Z_i = Z - 11$  for  $d$  electrons),  $F_r(j, Z_i)$  is a relativistic correction factor;  $\delta$  takes into account the finite charge distribution and  $\epsilon$  the distribution of the nuclear magnetic moment throughout the nuclear volume. The matrix element  $\langle r^{-3} \rangle$  is given by

$$\langle r^{-3} \rangle = \frac{Z_i}{a_0^3 n^{*3} l(l + \frac{1}{2})(l + 1)} \quad (7)$$

where  $n^* = Z_a (hcRy/E_b)^{1/2}$ ,  $E_b$  being the experimental binding energy and  $a_0$  the Bohr radius. The derivative  $dn^*/dn$  is obtained as the slope of a fit function  $n^* = n^*(n)$ . From these formulas one sees that the  $a$  factors are proportional to  $E_b^{3/2}$ , and that the hydrogenic model therefore predicts straight lines in a plot of  $\log a$  versus  $\log E_b$ .

Hyperfine splittings in alkali atoms are quite small (e.g., a few kilohertz at  $n \cong 20$  in Cs  $n^2D$  states) and relatively difficult to measure. Since the study of the hyperfine structure of heavy alkalis is not so difficult as for light alkalis, the number of states already investigated increases as one goes down in group I of the periodic table of elements. Although experimental results for highly excited states are not yet available, a number of states have already been investigated. The experimental data on K, Rb, and Cs were summarized in

the review papers of Belin *et al.* in 1975, 1976a, and 1976b, respectively. In the following emphasis will be given to the splitting of the D states. Such data have been obtained, e.g., by Farley *et al.* (1977) and Deech *et al.* (1977). Recently, Fredriksson *et al.* (1980) reported an investigation of the hyperfine structure of the  $5^2D_{3/2,5/2}^{133}\text{Cs}$ . As for many other alkali metal  $^2D$  states (Gupta *et al.*, 1972; Hogervorst and Svanberg, 1975; Belin *et al.*, 1976) the hyperfine splitting of the  $5^2D_{5/2}$  was found to be inverted, while that for the  $5^2D_{3/2}$  level was normal. From a theoretical point of view the  $5^2D$  states are quite interesting because they represent the lowest D states in cesium where relativistic effects can be expected to be important. The inversion of alkali metal atom  $^2D_{5/2}$  states was explained by Lindgren and co-workers (Lindgren *et al.*, 1976a,b). By using many-body perturbation theory very good agreement with experiment was obtained, especially for the  $4^2D_{5/2,3/2}$  states of rubidium (Lindgren, 1976b). While detailed inclusion of correlation effects is necessary for obtaining accurate theoretical values, the  $^2D_{5/2}$  state inversions are basically due to polarization effects induced in the core owing to the presence of the valence electron. Very recent results include measurements of the hyperfine structures of Cs  $15,16^2D_{3/2}$  (Nakayama *et al.*, 1981),  $nS_{1/2}$  and  $nP_{1/2}$  for  $23 \leq n \leq 28$  (Goy *et al.*, 1982) and the results of Na  $n^2P_{3/2}$   $5 \leq n \leq 9$  of Zhan-Kui *et al.* (1982). With the exception of the  $D_{5/2}$  states, all experimental results showed the expected linear behavior in a log-log plot of the magnetic dipole interaction constant versus binding energy as discussed above. This means that the hydrogenic model is able to describe the hyperfine structures, with the exception of the  $^2D_{5/2}$  states.

To describe the inversions of the  $^2D_{5/2}$  states, it is necessary to use a more refined model where several radial parameters are used to describe the hyperfine interactions. For D states the following expressions are obtained (Lindgren and Rosen, 1974):

$$a(^2D_{3/2}) = \frac{1}{10\pi} \mu_0 \mu_B^2 g'_I [6\langle r^{-3} \rangle_l + 2\langle r^{-3} \rangle_{sd} - \langle r^{-3} \rangle_c] \quad (8)$$

$$a(^2D_{5/2}) = \frac{1}{10\pi} \mu_0 \mu_B^2 g'_I [4\langle r^{-3} \rangle_l - 4\langle r^{-3} \rangle_{sd} - \langle r^{-3} \rangle_c]. \quad (9)$$

In these formulas  $\langle r^{-3} \rangle_l$ ,  $\langle r^{-3} \rangle_{sd}$ , and  $\langle r^{-3} \rangle_c$  are the orbital, spin-dipole, and contact radial parameters. By taking  $\langle r^{-3} \rangle_l = \langle r^{-3} \rangle_{sd} = \langle r^{-3} \rangle$  and  $\langle r^{-3} \rangle_c = 0$  the above formulas reduce to the hydrogen-like ones. By using, for example, many-body perturbation techniques it is possible to calculate individual values for the different radial parameters, considering polarization effects and correlation effects. For alkali D states core polarization effects are very strong, yielding a large  $\langle r^{-3} \rangle_c$ . In this way it is possible to explain the magnetic hyperfine structures of the anomalous D states (Lindgren *et al.*, 1976a;

Belin *et al.*, 1976; Svanberg, 1977) since this term appears with a negative coefficient in the formulas above. In special cases where the calculations have been performed to higher order, an agreement with experiment within a few percent is obtained (Lindgren *et al.*, 1976b).

### C. ALKALINE EARTH ATOMS

As seen in the previous section, high-resolution laser spectroscopy techniques have allowed one to obtain a rather good picture of phenomena occurring in alkaline atoms. In contrast, the Rydberg spectra of the alkaline earth atoms are much more complicated than those of the alkalis since the presence of two electrons in the open shell endows their Rydberg states with additional properties. Besides the Coulomb interaction between the electrons, the additional spin-spin contribution causes the appearance of Rydberg series with predominant singlet or triplet signatures. For bound-state Rydberg series only one of the valence electrons is excited and the configurations are of the type  $msnl$  ( $m = 4, 5,$  and  $6$  for Ca, Sr, and Ba, respectively). Furthermore, as is to be expected, the presence of doubly excited configurations will strongly perturb the series with one excited electron. As a consequence, one should expect to have singlet-triplet and/or configuration mixing more or less localized in energy. An example is the interaction between the levels of the  $6snd$  series for  $n \leq 40$  with levels of the  $5d6d$  and  $5d7d$  configurations in Ba (Rinneberg, 1984; Aymar, 1984). All the interactions between the various Rydberg series are described in the general framework of the multichannel quantum defect theory (MQDT) (Seaton, 1983; Fano, 1983).

The basic idea of MQDT lies in the observation that interactions between the electron and the ionic core can be separated into long-range and short-range effects. Far from the ionic core the effects are described by Coulomb radial eigenfunctions. Near the core, where interactions are stronger, one uses eigenfunctions which are characterized by two sets of parameters: quantum defects  $\mu_\alpha$  and matrix elements  $U_{i\alpha}$ , which describe the change of coupling between the electron and the core as their distance changes. One then speaks of "collision channels"  $i$  and of "close-coupling channels"  $\alpha$ . The former correspond to the asymptotic Coulomb eigenfunctions, while the latter describe the state of the inner region. The problem then consists of connecting the collision channels  $i$  and the close-coupling channels  $\alpha$ , i.e., of determining the "mixing coefficients." These mixing coefficients depend on the two sets of parameters  $\mu_\alpha$  and  $U_{i\alpha}$  and are expected to vary only weakly with the energy. The values of these parameters may be either calculated *ab initio* or derived from a numerical analysis of perturbed Rydberg series

through the so-called Lu–Fano plots. Up to now only this latter empirical fitting approach has been used to analyze heavy alkaline earth spectra and to obtain the two sets of parameters. The parameter  $\mu_\alpha$  and  $U_{i\alpha}$  allow eigenfunctions for each individual Rydberg level to be constructed. The eigenfunctions obtained in this way cannot be uniquely determined if only the level energies are known experimentally. Additional experimental data such as hyperfine structure, isotope shifts, radiative properties, and interactions of individual Rydberg levels with external fields are therefore very much needed in order to determine the eigenfunctions unambiguously and use them to predict new properties (Aymar, 1984).

In 1980, using a relatively broad-band laser (50 MHz), Barbier and Champeau reported a systematic study of hyperfine structures as well as isotope shifts of  $6snd\ ^3D_1$  Rydberg states of Yb. Simultaneously, Liao *et al.* (1980) reported a complete determination of the hyperfine structure of  $2\ ^3P$  and of  $3\ ^3D$  states of  $^3\text{He}$  in which significant singlet–triplet mixing was observed. They identified the mixing as arising from the hyperfine interaction of the  $1s$  open-shell electron and the interaction as being basically independent of the outer electron. These results are very clear indications that the hyperfine structure of excited state atoms with two valence electrons is very sensitive to state mixing.

At present, the hyperfine structure and isotope shifts of Ca, Sr, and Ba [as well as the Group IIB (Zn, Cd, Hg) and even the Group III elements (Belfrage *et al.*, 1983)] are being extensively studied, mainly by very active groups in Amsterdam, Berlin, Göteborg, Kiel, and Lund. In all cases the hyperfine structure of single excited Rydberg states, i.e., of configurations like  $msnl$  is dominated by the strong Fermi contact interaction between the nuclear magnetic dipole moment and the innermost  $ms$  valence electron. As for alkalis, the contribution of the  $n/l$  Rydberg electron decreases as  $n^{*-3}$  and, in virtually all cases can be neglected. It is therefore possible to resolve the hyperfine structure of the  $msnl$  Rydberg states, even for high  $n$ , while much higher precision is needed to measure hyperfine structures of Rydberg states of alkali-type systems. As mentioned before, the correlation energy between the two valence electrons is very important in the study of the hyperfine structure of two-electron atoms. Indeed, singlet and/or triplet character is important for the magnetic properties of Rydberg states and hyperfine measurements are very direct and particularly sensitive ways of determining singlet–triplet mixing.

In Table IV we present detailed references on hyperfine data already available for two-electron systems. As the excitation of the outer electron increases, the hyperfine coupling of the  $ms$  electron remains essentially constant while singlet–triplet separations and fine-structure splittings of  $msnl$  Rydberg states decrease proportionally to  $n^{*-3}$ . Eventually (when the

TABLE IV

RESULTS ON HYPERFINE STRUCTURES OF ALKALINE EARTH RYDBERG ATOMS

Element	Series	$n$	Reference	
Ca	4sns	$^1S_0$	Up to 21	Beigang <i>et al.</i> (1982a)
	4snd	$^1D_2$	$7 \leq n \leq 42$	Beigang <i>et al.</i> (1983)
Sr	5sns		Up to $\sim 180$	Beigang and Timmermann (1982a,b)
	5snd			Beigang and Timmermann (1983)
	5s6p	$^1,^3P_1$		Eliel <i>et al.</i> (1983)
	5snd	$^1,^3D_2$	Up to $\sim 70$	Beigang <i>et al.</i> (1981)
Ba	5d7d	$^1D_2$		Rinneberg and Neukammer (1982a)
	6sns	$^1S_0$	$11 \leq n \leq 50$	Rinneberg <i>et al.</i> (1983)
		$^1S_0$	$21 \leq n \leq 50$	Beigang and Timmermann (1982a)
		$^3S_1$	$14 \leq n \leq 23$	Neukammer and Rinneberg (1982a)
		$^3S_1$	15-18, 20	Hogervorst and Eliel (1983)
	6s6p	$^1P_1$		Neukammer and Rinneberger (1982b)
	6s7p	$^1P_1$		Eliel <i>et al.</i> (1983)
	6snd	$^1D_2$	$10 \leq n \leq 50$	Rinneberg and Neukammer (1982b; 1983)
		$^1D_2$	$12 \leq n \leq 24$	Grafström <i>et al.</i> (1982)
		$^3D_2$	$11 \leq n \leq 27$	Neukammer and Rinneberg (1982c)
		$^1,^3D_2$	Up to 20	Eliel and Hogervorst (1983a)
	6snf		$4 \leq n \sim 30$	Eliel and Hogervorst (1983b)

Fermi contact interaction is about of the same order as the fine-structure splittings), strong mixing between *msnl* fine-structure components (corresponding to a recoupling of the several components of the total angular momentum *F*) provokes not only shifts but also intensity variations in the observed hyperfine spectra. For high enough *n*, even hyperfine-induced *n* mixing can occur (Beigang and Zimmermann). As is obvious, besides singly excited Rydberg states, both valence electrons might occupy higher orbits. Such doubly excited states may strongly perturb *msnl* Rydberg series by configuration interaction, displacing the Rydberg levels and causing intensity variations.

### VI. Interactions of Rydberg Atoms with Blackbody Radiation

The effect of blackbody radiation on Rydberg atoms is mainly to induce transitions to nearby states. As a result the population will evolve as a function of time after pulsed laser excitation. Changes in the populations typically appear on a microsecond time scale. The most straightforward way

of proving that blackbody radiation affects the Rydberg atoms is to vary the temperature of the environment. Experimentally, this requires a careful design of the interaction chamber so that no radiation leaks into the chamber. In the first experimental verification of blackbody radiation effects Gallagher and Cooke (1979) therefore did not vary the temperature but measured the lifetime of high-lying p states of Na and found values three times smaller than theoretically predicted. When, however, room-temperature blackbody-induced population transfer to nearby states is included, good agreement with the experimental data was achieved.

Haroche *et al.* (1979) observed that the decay of the 25s sodium state occurs with an important population transfer to nearby states, such as the 25p level, which cannot be accounted for by ordinary spontaneous emission (since the 25p level lies above the 25s one). This transfer of population can be quite consistently explained as a 20% blackbody radiation-induced mixing between the 25s and 25p states.

In a slightly different approach Beiting *et al.* (1979) used field ionization of Rydberg atoms with a linearly rising electric field pulse. As described in Section III, different Rydberg states ionize at different electric field strengths. With such a set-up, the population distribution among the Rydberg states can be measured in a single shot. Beiting *et al.* (1979) measured this population distribution for various delays between the pulsed laser excitation and the ionizing electric field pulse. It was observed that the population initially prepared in one Rydberg state is transferred to higher lying states, the more the longer the delay. Using a similar set-up, Rempe (1981) measured the population transfer from the initially laser-excited  $23^1F_3$  state of strontium to nearby d and g states (Fig. 5). In these experiments the temperature of the environment was again not varied. However, it was carefully checked that the population transfer is due to the blackbody radiation.

The first direct observation of the temperature dependence of the population transfer was performed by Koch *et al.* (1980) by heating the environment, and in an experiment by Figger *et al.* (1980) where sodium atoms of a thermal beam in a cooled environment were excited to the 22d state using two continuous wave (cw) dye lasers. In the latter case the interaction region was inside a copper box cooled to 14 K (Fig. 6). The sodium Rydberg atoms could be exposed to the radiation of a blackbody source by opening a flap at the side of the box. After interacting with the blackbody radiation for about 50  $\mu$ sec the atoms entered a dc electric field which acted like an optical edge filter: all atoms in Rydberg states higher than the initially laser-excited 22d state are ionized and detected. Figure 7 shows the ionization signal for different temperatures of the blackbody source. The signal rises linearly with temperature, in good agreement with the Rayleigh–Jeans limit of Planck's

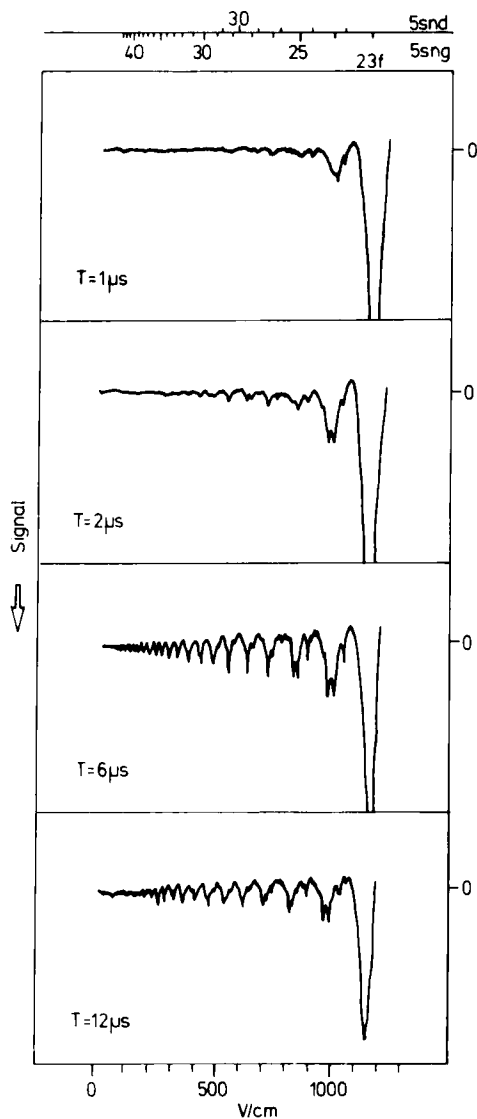


FIG. 5. Blackbody-induced transitions between Rydberg states. The  $23\ ^1F_3$  level of strontium is excited by the laser radiation. The detection of the Rydberg states is performed by an electric field increasing linearly in time. The field ramp starts 1, 2, 6, and  $12\ \mu\text{sec}$  after the pulsed laser excitation. The field ionization signal at smaller field strengths results from Rydberg levels populated by blackbody radiation of the apparatus at 300 K.

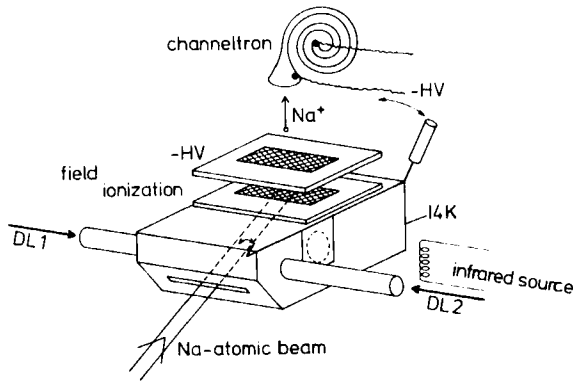


FIG. 6. Experimental set-up for demonstrating the interaction of blackbody radiation with Rydberg atoms. The flap at the right side of the cooled box (14 K) allows the thermal radiation of the infrared source to enter the box. The  $22d$  state was excited by cw laser radiation. The Rydberg atoms in the  $22p$  level were detected by field ionization.

radiation formula. The effect of the blackbody source mounted outside the box is reduced since the atoms only see the source at a small solid angle.

Aside from population transfer, blackbody radiation also affects Rydberg atoms in a more subtle way. The spectral energy density distribution of the blackbody radiation at 300 K has its maximum at about  $2 \times 10^{13}$  Hz. A typical electric dipole transition starting from the ground state of an atom has  $10^{14} - 10^{15}$  Hz and a transition between two Rydberg states has about  $10^{11}$  Hz. It is thus apparent that for a ground-state atom the blackbody radiation appears as a slowly varying field, whereas for a Rydberg atom it appears to be rapidly varying leading to an ac Stark shift of the Rydberg levels. The black-

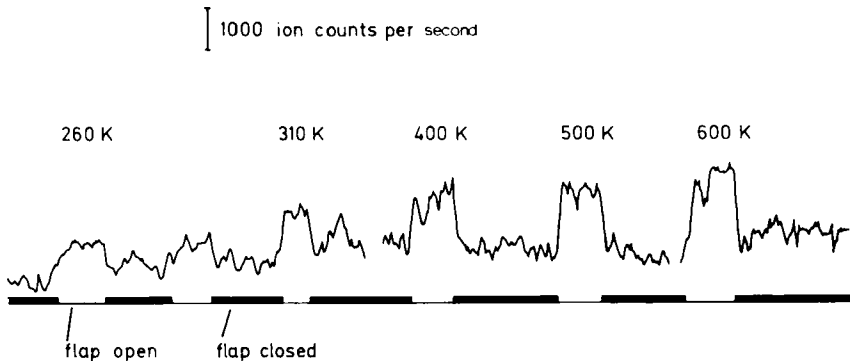


FIG. 7. By opening and closing the flap (see Fig. 6) the ion signal is changed. The background (not shown in the figure) is about five times the signal induced by the infrared source at 310 K and is due to the 14 K blackbody radiation emitted by the walls of the box.

body-induced ac Stark shift  $\Delta W_n$  for a Rydberg atom in the state  $n$  can be expressed as (Townes and Schawlow, 1955)

$$\Delta W_n = \frac{e^2}{2h} \sum_{n'} \int_0^\infty \frac{\langle r_{nn'} \rangle^2 E_{\omega_b}^2 \omega_{nn'}}{(\omega_{nn'} - \omega_b)(\omega_{nn'} + \omega_b)} d\omega_b \quad (10)$$

where  $E_{\omega_b}^2$  is the squared electric field of the blackbody radiation in a band width  $d\omega_b$  at a frequency  $\omega_b$ . Accurate evaluation of the shift was performed by Farley and Wing (1981). A rather good estimate is obtained when it is assumed that the frequencies of the strong transitions are much lower than the frequency of the blackbody radiation, i.e.,  $\omega_{nn'} \ll \omega_b$ , which is generally fulfilled for the Rydberg states (Cooke and Gallagher, 1980; Gallagher *et al.*, 1981). Under this condition the  $\omega_{nn'}$  in the denominator of Eq. (3) can be neglected and one obtains

$$\Delta W_n = \left( \sum_{n'} f_{nn'} \right) \left( \frac{e^2}{m} \int_0^\infty \frac{E_{\omega_b}^2 d\omega_b}{4 \omega_b^2} \right) \quad (11)$$

If the oscillator strength sum rule  $\sum f_{nn'} = 1$  is used and the integral is evaluated, Eq. (11) may be expressed as

$$\Delta W_n = \pi\alpha(kT)^2/3mc^2 \quad (12)$$

where  $\alpha$  is the Sommerfeld fine-structure constant. The comparison of the results obtained with this formula to the accurate results of Farley and Wing (1981) gives a deviation of about 10% for  $n > 15$  at 300 K. All Rydberg states experience roughly the same energy shift of about 2.4 kHz at 300 K.

Since the shift of all Rydberg states by blackbody radiation is the same, it can be detected only as a change of the optical transition frequency which connects to the ground state. Consequently, the line width and the stability of the dye laser used for excitation has to be  $10^{-12}$  and the spectral resolution in the experiment has to be correspondingly high. This challenge was accepted by Hollberg and Hall (1983). They used Doppler-free two-photon absorption to excite the 5s–36s transition in rubidium atoms. With the Ramsey method of separate fields, the spectral width of the signal was decreased to 40 kHz. The line center could be determined with an accuracy of 150 Hz. The atoms were exposed to the radiation of a blackbody source, and a chopper periodically blocked this radiation. Thus, the experiment was insensitive to long-term drifts. When the temperature of the blackbody source was raised to about 500 K, a shift in the line position of 1.4 kHz was observed. This is 10 times larger than the uncertainty. A first study of the temperature dependence also shows agreement with the predicted  $T^2$  dependence.

Gallagher *et al.* (1981) measured the blackbody radiation-induced level

shift in two-electron atoms where a state of a doubly excited configuration has an energy so close to a singly excited Rydberg state that the transition frequency is in the microwave region. Since the doubly excited state is not shifted by the blackbody radiation, the shift of the Rydberg state is measurable at the comparatively low microwave frequency. As pointed out by Gallagher *et al.* (1981), the measurement of blackbody-induced level shifts may in turn also be used to determine the absolute temperature of the environment. See Section I,C (H.R.) for further discussion of this interesting topic.

## VII. Radiation Interaction of Rydberg Atoms — A Test System for Simple Quantum Electrodynamical Effects

The invention of the maser has generated a great deal of interest in theoretical models describing the interaction of two-level atoms with a single mode of an electromagnetic field (e.g., Jaynes and Cummings, 1963; Allen and Eberly, 1975; Knight and Milonni, 1980). Although the first models treated a purely academic problem, modified versions were stimulated. These then led to an understanding of a major part of the experimentally observed phenomena, including the even larger variety of effects found after the laser was invented. In the experiments on atoms in low-lying states it is always necessary that large numbers of atoms and photons are present. This is due to the fact that the matrix elements describing the interaction between radiation and atoms are small. A small number of photons in an experiment has the consequence that the atom–field evolution time indeed usually becomes much longer than other characteristic times such as the atomic relaxation, the atom–field interaction time, and the cavity mode damping time. The theories involving single electromagnetic modes and small photon occupation numbers are therefore not very realistic. They, however, predict some interesting and basic effects. Among them are the following:

- (1) Modification of the spontaneous emission rate of a single atom in a resonant cavity.
- (2) Oscillatory energy exchange between a single atom and the cavity mode.
- (3) Disappearance and quantum revival of optical nutation induced on a single atom by a resonant field.

Rydberg atoms are very suitable for observing these effects for several reasons: They have a very strong coupling to the radiation field, as already mentioned; the transitions to neighboring levels are in the region of millimeter waves, which allows one to build cavities with low-order modes that are reasonably large to ensure rather long interaction times; finally, the Rydberg atoms have long spontaneous emission times, and therefore only the interaction with the selected cavity mode is important and the coupling of the atoms to other cavity modes can be neglected.

In the following, several phenomena observable with Rydberg atoms are discussed in more detail.

#### A. SINGLE ATOM IN RESONANT CAVITY—MODIFICATION OF SPONTANEOUS EMISSION RATES

The energy levels of the combined two-level atom and field system can be described in the dressed atom picture (Haroche, 1971; Haroche *et al.*, 1982). The lowest energy of the system is represented by  $|g,0\rangle$  describing the atom in its ground state  $|g\rangle$  with no photon in the cavity. The higher energy levels are separated by the energy of a photon. The states  $|\pm n\rangle$  are a superposition of the states  $|e,n\rangle$ , ( $e$  stands for excited atomic state and  $n$  for the photon number) and  $|g,n+1\rangle$  of the system without interaction between the cavity field and the atom:

$$|\pm n\rangle = [|e,n\rangle \pm |g,n+1\rangle]/\sqrt{2} \quad (13)$$

The energy separation between the levels  $|+n\rangle$  and  $|-n\rangle$  is  $2h\Omega\sqrt{n+1}$ , where  $\Omega$  is the coupling strength between the field and the atoms. There is a small change proportional to  $\sqrt{n}$  when the field strength is increased. The energy levels of the dressed atom taking the coupling with the field into account are shown in Fig. 8.

In a realistic description of the interaction the dissipative processes also have to be considered. Since Rydberg atoms have lifetimes longer than the atom-field interaction time, their relaxation can generally be neglected. However, the relaxation of the cavity field is important: the harmonic oscillator representing the field is coupled to a thermal reservoir at temperature  $T$  representing, for example, the cavity walls. The scheme shown in Fig. 9 gives the corresponding "coupling constants." The thermal equilibrium of the field mode is obtained in the characteristic time  $Q/\omega$ , where  $Q$  is the quality factor of the cavity and  $\omega$  the frequency of the resonant mode.

The behavior of an atom entering an empty cavity (i.e., at  $T = 0$  K) in the excited state  $|e\rangle$  depends on the relative size of  $\Omega$  and  $\omega/Q$ . If  $\Omega > \omega/Q$  (small damping of the cavity), the probability of finding the atom in the state  $|e\rangle$

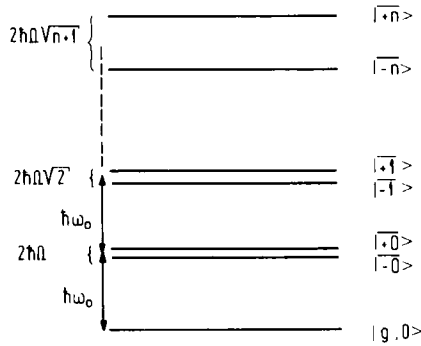


FIG. 8. Energy levels of a single two-level atom in the dressed atom description with resonant coupling to a cavity mode.

undergoes a damped oscillation. This regime can be considered as a self-induced Rabi nutation in the field of the single photon emitted and reabsorbed by the atom. If  $\Omega < \omega/Q$ , the probability decreases exponentially at a rate  $\Gamma_{\text{cavity}} = 4 \Omega^2 Q/\omega$ . There is a cavity-enhanced decay rate which is related to the spontaneous rate in free space  $\Gamma_{\text{spont}}$  in the following way:

$$\Gamma_{\text{cavity}} = (3/4\pi^2) \cdot Q\lambda^3 \Gamma_{\text{spont}}/V \tag{14}$$

where  $V$  is the volume of the cavity and  $\lambda$  the wavelength of the radiation.

This relation was predicted long ago by Purcell (1946). Physically, the cavity enhances the strength of the vacuum fluctuations at the resonance frequency; as a consequence the transition rate is increased. ( $\Gamma_{\text{cavity}}/\Gamma_{\text{spont}}$  is obtained when the number of oscillator modes per unit frequency interval in a resonant cavity is divided by the corresponding value in free space.)

The opposite effect, the decrease of the decay rate, is obtained when the cavity is detuned. If the transition frequency of the atom lies below the fundamental frequency of the cavity, spontaneous emission is significantly inhibited. In an ideal case no mode is available for the photon and therefore spontaneous emission cannot occur (Kleppner, 1981).

To change the decay rate of an atom, in principle no resonator has to be present; any conducting surface near the radiator affects the mode density and, therefore, the radiation rate. Parallel-conducting planes can somewhat

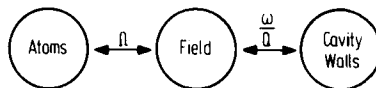


FIG. 9. Schematic description of the atom-single field mode system. The coupling is described by the one-photon Rabi frequency  $\Omega$  and the characteristic damping time  $Q/\omega$ .

alter the emission rate but can only reduce the rate by a factor of 2 because of the existence of TEM modes, which are independent of the separation. The effect of conducting surfaces on the radiation rate has been studied theoretically in a number of investigations (Purcell, 1946; Milonni *et al.*, 1973; Wittke, 1975; Kleppner, 1981).

To demonstrate experimentally the modification of the spontaneous decay rate, it is not necessary to go to single-atom densities in both cases. The experiments where the spontaneous emission is inhibited can also be performed with higher densities. However, in the opposite case, when the increase of the spontaneous rate is observed, a large number of excited atoms increases the field strength in the cavity and the induced transitions disturb the experiment.

The first experimental work on the inhibited spontaneous emission was done by Drexhage (1974). The fluorescence of a thin dye film near a mirror was investigated. Drexhage observed an alteration in the fluorescence lifetime arising from the interference of the molecular radiation with its surface image. An experiment with Rydberg atoms was recently performed by Vaidyanathan, Spencer, and Kleppner (1981). They observed a wavelength-dependent cutoff in the absorption of blackbody radiation by Rydberg atoms arising from a discontinuity in the density of modes between parallel-conducting plates. Absorption at a wavelength of  $\frac{3}{2}$  cm by atoms between planes  $\frac{1}{2}$  cm apart was measured at a temperature of 180 K. The discontinuity in the absorption rate occurred when the absorption wavelength was varied across the cutoff of the parallel-plate modes. The experiment was performed with Na atoms and the transition employed was  $29d \rightarrow 30p$ . For the tuning of the atomic resonance across the cutoff frequency a small electric field was applied to the parallel plates.

Inhibited spontaneous emission was observed clearly for the first time by Gabrielse *et al.* (1984) and by Gabrielse and Dehmelt (1984). In these nice experiments on a single electron stored in a Penning trap they observed that the cyclotron excitation shows a lifetime which is up to 10 times larger than that calculated for a cyclotron orbit in free space. The electrodes of the trap form a cavity which decouples the cyclotron motion from the vacuum radiation field leading to a longer lifetime.

The first observation of enhanced atomic spontaneous emission in a resonant cavity was published by Goy, Raimond, Gross, and Haroche (1983). Their experiment was performed with Rydberg atoms of Na excited in the  $23s$  state in a niobium superconducting cavity resonant at 340 GHz. Cavity tuning-dependent shortening of the lifetime was observed taking advantage of the very strong electric dipole of these atoms and of the high  $Q$  value of the superconducting resonator. This cooling, necessary for superconducting operation, also had the advantage of totally suppressing the blackbody field

effects ( $n = 0$ ) required to test purely spontaneous emission effects in the cavity (see Haroche and Raimonde, this volume, Section III, B, 3.)

It was shown that the partial spontaneous emission probability on the  $23S \rightarrow 22P$  transition in Na is increased from its free space value  $\Gamma_{\text{spont}} = 150 \text{ sec}^{-1}$  up to  $\Gamma_{\text{cavity}} = 8 \times 10^4 \text{ sec}^{-1}$ . This enhanced rate is still 35 times smaller than the damping rate  $\omega/Q = 2.8 \times 10^6 \text{ sec}^{-1}$  of the field in the cavity. This means that the photon emitted in the mode is absorbed in the mirrors much faster than the atoms decay.

With a 10-fold increase in  $Q$ , the values of  $\Gamma_{\text{cavity}}$  and  $\omega/Q$  would be of the same size, so that the emitted photon would be stored in the cavity long enough for the atom to reabsorb it. This would approach the regime of quantum mechanical oscillations between a two-level atom and a single electromagnetic field mode mentioned at the beginning of this section. The self-induced single-photon Rabi nutation is much more difficult to observe than the collective Rabi oscillation (which will be described later) because it occurs at a rate  $\sqrt{N}$  times smaller ( $N$  is the number of atoms in the cavity) and thus requires the atom to be kept in the cavity for much longer times. Experiments to observe this single-atom – single-photon interaction are presently under way at the École Normale Supérieure in Paris and in our laboratory. The set-up used in our laboratory (Meschede, 1984) is shown in Fig. 10.

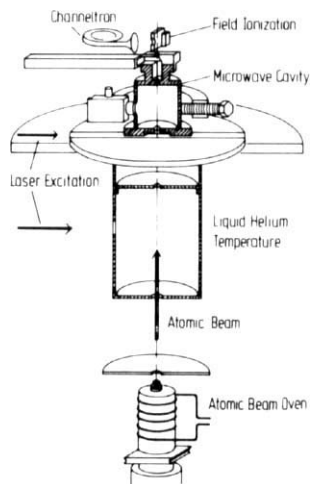


FIG. 10. Experimental set-up for observation of single-atom–single-photon interaction. The Rydberg atoms are prepared in a specific velocity subgroup by a modulated stepwise excitation either with two laser beams or with modulated laser and microwave fields. (The figure shows the position of two laser beams.) The length of the cylindrical cavity is about 20 mm. The microwave cavity and the surrounding parts are cooled to 2 K with liquid helium (figure according to Meschede, 1984).

The superconducting niobium cavity has a  $Q$  value of  $8 \times 10^8$ . In this experiment the atoms are velocity selected during the stepwise excitation into the Rydberg states by using the modulated radiation of two lasers. Instead of the second laser a modulated microwave field can also be used in order to prepare a selected velocity subgroup. The latter method has the advantage that the first excitation step can already be performed into a Rydberg state with high  $n$  and long radiative lifetime. This reduces the losses due to spontaneous decay between the two excitation regions.

With the set-up shown in Fig. 10 maser oscillation with single atoms was recently observed (for the first experiments the velocity selection of the atoms described above was not operational). The transition  $63p_{3/2} - 61d_{3/2}$  at about 21.5 GHz between  $^{85}\text{Rb}$  Rydberg states was used. The atoms of a beam were excited by the frequency-doubled light of a cw dye laser. The cavity was operated in the  $\text{TE}_{121}$  mode. Its high  $Q$  value of  $8 \times 10^8$  allowed us to observe maser oscillation with an average number of atoms in the cavity of only 0.06. An increase in the density of the atoms caused power broadening of the transition and ultimately for about one atom also caused a dynamic Stark shift (Fig. 11). The experiments clearly show that the set-up should also be suitable for observing the predicted quantum revival (see next section). For this observation the interaction time of the atoms with the cavity field has to be well defined and therefore a velocity selection of the atoms in the thermal beam is necessary. Experiments along these lines are at present under way.

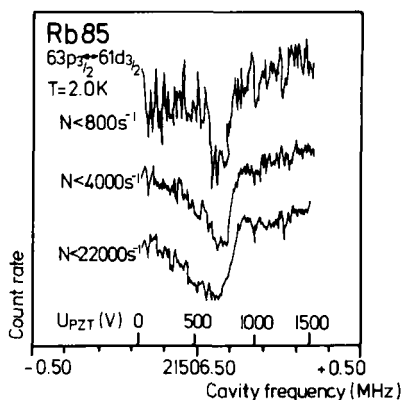


FIG. 11. Maser operation with single atoms. Shown is the signal of the atoms in the  $63p_{3/2}$  level when the cavity is tuned through the resonance for the  $63p_{3/2} - 61d_{3/2}$  transition of  $^{85}\text{Rb}$ . The flux of the beam is changed for the three curves. The three curves from top to bottom correspond to only 0.06, 0.30, and 1.6 atoms being simultaneously in the cavity.

### B. SINGLE ATOM IN RESONANT CAVITY—DISAPPEARANCE AND REVIVAL OF OPTICAL NUTATION

At temperatures  $T > 0$  K the cavity also contains thermal photons. The effects described above therefore become more complicated since the atom evolves through an oscillatory or irreversibly damped transient regime toward a final state distribution corresponding to the thermal equilibrium. The transient behavior is again dependent on whether there is weak ( $\Omega \gg \omega/Q$ ) or strong damping ( $\Omega \ll \omega/Q$ ) of the cavity. In the first case the transient regime can be described by a sum of elementary Rabi oscillations in a field in which the number of photons is a random quantity following the Bose–Einstein statistics. The distribution of Rabi frequencies results in an apparently random oscillation which for large  $n$  values very quickly collapses and then revives again (Faist *et al.*, 1972; Meystre *et al.*, 1975; Eberly *et al.*, 1980; Knight and Radmore, 1982, 1983). This behavior is typical of a chaotic quantum field; a semiclassical description of a random Gaussian field does not give this result. It has always been thought that this interesting phenomenon could not be observed experimentally. However, the possibilities now opened up by Rydberg atoms bring us close to its realization. Superconducting cavities with  $Q$  values in the range between  $10^9$  and  $10^{10}$  can be realized and, therefore, it should be possible to keep the damping small enough so that the oscillations are not washed out before their revival occurs.

### C. $N$ ATOMS IN RESONANT CAVITY—COLLECTIVE BEHAVIOR

The generalization of the single-atom effects described in the previous sections to  $N$  two-level atoms can be based on the ladder of equidistant nondegenerate states, the so-called symmetrical Dicke states (Dicke, 1954).

Such a state, where  $J + M$  atoms are excited in level  $|e\rangle$  and  $J - M$  in level  $|g\rangle$ , is written formally

$$|JM\rangle = S \underbrace{|e, e, \dots, e\rangle}_{J+M} ; \underbrace{|g, g, \dots, g\rangle}_{J-M} \quad (15)$$

where  $S$  is the symmetrization operator. ( $M = J$  and  $M = -J$  correspond to the totally excited and de-excited states, respectively.) The analysis of the atomic system by Dicke states is related to the atomic indiscernibility with respect to the single mode of the cavity. The  $N + 1$  states  $|JM\rangle$  describe situations in which strong correlations exist between the dipoles of different atoms, resulting in collective behavior of the atoms in the cavity. Again, the

strong atom-to-field coupling of the Rydberg atoms is a big advantage, so that the experimental verification of the phenomena is much simpler than for "ordinary" atoms. The effects observed are cooperative features which cannot be interpreted in terms of an independent atom model: collective oscillations and superradiance, when the system is initially in the upper level, and collective absorption, when the system starts in the lower level.

For discussion of the phenomena one has again to consider the two cases where either the collective Rabi frequency  $\sqrt{N}\Omega$  is either larger or smaller than the reciprocal of the cavity damping time  $\omega/Q$ . In the case without blackbody photons ( $T = 0$  K), with  $\omega/Q = 0$ , and with all the atoms in the excited state, the spontaneous emission causes the atomic system to cascade through the ladder of eigenstates. The field strength in the cavity is increased and the photons are reabsorbed. The subsequent oscillations can be interpreted as a Rabi nutation in the field radiated by the atoms and stored in the cavity (Bonifacio and Preparata, 1970; Scharf, 1970). The oscillations show a rather complicated beating pattern for small  $N$  values (Haroche, 1982).

For large  $N$  values, the number of states to keep track of becomes prohibitive. Fortunately, the system can then be described in a classical way by using the concept of the Bloch vector (see, for example, Allen and Eberly, 1975; for the relation between the quantum mechanical and Bloch vector approaches see, for example, Bonifacio *et al.*, 1969).

In the case of strong cavity damping the energy decays with a rate  $T_R^{-1} = 4 \Omega^2 N Q / \omega$  (Bonifacio and Preparata, 1970). The value corresponds to  $N \cdot \Gamma_{\text{cav}}$ , where  $\Gamma_{\text{cav}}$  is the single-atom cavity-enhanced decay rate as discussed in the previous section.

The experimental observation of the above-mentioned effects was performed by Haroche and co-workers with an atomic beam of alkalis excited by pulsed lasers in the Rydberg states. A millimeter-wave transition involving either the upper or the lower level was in resonance with a mode of a cavity surrounding the atoms. The relatively long wavelength of the transitions allows all atoms to be excited in a region of constant field amplitude. The Rydberg atoms are monitored by field ionization after the atoms have passed the cavity. In this way the number of atoms in the upper or the lower level of the microwave transitions was measured. In order to reconstruct the atomic evolution during the time the atoms spend in the cavity, a small electrode producing an inhomogeneous electric field at a present time  $t$  was inserted into the cavity. The Stark shift produced by this field suddenly brings the atoms out of the cavity resonance. A scheme of the experimental set-up is shown in Fig. 12. The atom-cavity coupling is therefore interrupted and the detector measures the state the atom had at time  $t$ . The dynamics of the atom-cavity interaction can be reconstructed by varying  $t$ .

Actual experiments were performed with cavities at  $T = 300$  K whereas

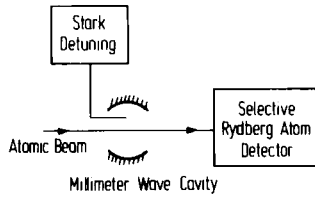


FIG. 12. Schematic of the Rydberg atom-cavity experimental set-up. The millimeter-wave cavity is made of spherical copper mirrors. (For details and references see text.)

the theories deal with systems at  $T = 0$  K. In fact, it can be shown that, as long as  $N$  is larger than the number of blackbody photons in the cavity, the thermal field contributions rapidly become negligible (Raimond *et al.*, 1982b). Blackbody effects are relevant only at the onset of the emission, when the emitted field is still much smaller than the thermal one. With respect to fluctuations there is no difference since thermal and vacuum fields have the same statistical nature.

The experiments in a moderate  $Q$  cavity, typically  $Q \approx 10^4$  (Moi *et al.*, 1983; Raimond *et al.*, 1982b), give the predicted cavity-assisted overdamped superradiance. This superradiant Rydberg “maser” is characterized by an extremely low inversion density threshold ( $N \sim 10^4$  atoms). The inverted medium emits a short burst of radiation and decays within a few hundred nsec to the lower state of the transition (in the experiments mostly  $n S_{1/2} \rightarrow (n-1) P_{1/2,3/2}$  or  $n S_{1/2} \rightarrow (n-2) P_{1/2,3/2}$ ,  $n \approx 30$ ). This maser emission was also detected by using Schottky heterodyne receivers (Moi *et al.*, 1980, 1983). The latter detection technique is of course considerably less sensitive than the one based on atomic field ionization, which actually allows one to count the atoms which have radiated inside the cavity during a given time interval and hence the emitted photons. Such a photon-counting type of experiment is quite novel in this part of the radiation spectrum.

Raimond *et al.* (1982b, 1983) succeeded in measuring the probability distribution  $P(n,t)$  that  $n$  atoms have been de-excited at time  $t$  (see Haroche and Raimond, this volume, Section IV,C).

As discussed above, in the high  $Q$  regime ( $Q \approx 10^6$ ) one expects to observe an oscillatory exchange of energy between the atoms and the cavity field which can be described as a self-induced Rabi nutation of the atomic system. The experimental observation was performed by Kaluzny *et al.* (1983). The transition investigated was  $36 S_{1/2} - 35 P_{1/2}$  of the Na atom. In order to remove the twofold degeneracy in the upper and lower levels and to study a true two-level atom transition, a small dc magnetic field was applied along the cavity axis and the cavity is tuned to resonance with  $36 S_{1/2}$ ,  $m_J = +1/2 \rightarrow 35 P_{1/2}$ ,  $m_J = 1/2$  transition at about 82 GHz.

The emission of the  $N$  atoms in the cavity occurs faster than it would in

free space, essentially owing to the cavity enhancement effect. When  $N$  was sufficiently high ( $N > 20,000$ ), oscillations in the atomic population evolution becomes clearly observable. This collective self-nutation regime has also been discussed in the context of superradiance theories (Bonifacio *et al.*, 1975; McGillivray and Feld, 1976; Haake *et al.*, 1979; Polder *et al.*, 1979). It is then generally referred to as the “ringing” regime of superfluorescent emission. In the case of free-space superradiance this phenomenon has not yet been clearly observed since the simple Rabi nutation is then masked by multimode diffraction and propagation effects.

#### D. $N$ ATOMS IN RESONANT CAVITY—COLLECTIVE ABSORPTION OF BLACKBODY PHOTONS

In the previous section the case where the  $N$  atoms were initially in the excited Dicke state  $|J, +J\rangle$  was discussed. In the following, the  $N$  atoms are now assumed to enter the cavity in the lowest state  $|J, -J\rangle$ ; furthermore, it is assumed that the cavity field is in thermal equilibrium at a temperature  $T \neq 0$  K.

The thermal photons represent a Bose–Einstein distribution with an average photon number  $\bar{n} \neq 0$ . As the time evolves, the atoms gain energy at the expense of the mode which is then supplemented by the thermal reservoir. The time constant for reaching thermal equilibrium depends on the values of  $N$ ,  $\bar{n}$ , and  $\omega/Q$ . Since the atomic energy diagram consists of nondegenerate equidistant levels with the same spacing as the field levels, the atoms will obviously reach an equilibrium described by a Boltzmann law quite similar to the Bose–Einstein distribution of the photon number in the field mode. (The only difference between the two distributions is that the number of levels for the atomic system is finite; this changes the normalization of the Boltzmann distribution.) As a consequence, the number of absorbed photons  $\Delta N$  is limited, no matter what value  $N$  has, and is equal to the average blackbody photon number per mode (as soon as  $N > \bar{n}$ ):

$$\Delta N = \bar{n} = [\exp(h\omega/kT) - 1]^{-1} \quad (16)$$

which is close to  $kT/h\omega$  in the Rayleigh–Jeans limit.

The energy absorbed by  $N$  atoms in the cavity is not identical with the sum of energy that would be absorbed by  $N$  independent atoms. In this process the atomic sample evolves in a collective mode and behaves as a single quantum system exhibiting basic effects of Bose–Einstein statistics and Brownian motion (Raimond *et al.*, 1982a). A detailed study of the pulse-to-pulse random variations of  $\Delta N$  around  $\Delta \bar{n}$  should allow one to probe the fluctuations of the cavity mode and to reconstruct their Bose–Einstein

distribution. There is a connection between the absorption and emission of  $N$  atoms in a cavity: The atomic indiscernibility, which is responsible for superradiance when the system is initially excited, leads to a kind of "subabsorption" (Raimond *et al.*, 1982a) when it starts from its lower state.

The experimental demonstration of the effects just described was first performed by Raimond *et al.* (1982a); see Haroche and Raimond, this volume, Section IV,C, for a detailed discussion.

## VIII. Rydberg States of Molecules

Compared with the great amount and large variety of work performed on Rydberg states of atoms there are very few studies on highly excited states of molecules. This is the result of the great complexity of the absorption and emission spectra caused by the vibrational and rotational structure in addition to the closely spaced Rydberg levels. Selective excitation of the highly excited levels is almost impossible owing to the thermal population of the rotational and vibrational levels of the electronic ground state. This is the reason why in many investigations the molecules are cooled to low temperatures or why molecular beams with nozzle expansion are used, which cools down the internal degrees of freedom.

The new methods of laser spectroscopy are also of great help in simplifying the complex spectra, so that more and more studies have been published in recent years.

The Rydberg levels of diatomic molecules show some very interesting peculiarities. A molecular Rydberg level can lie above the lowest level of the corresponding molecular ion and can autoionize if part of the vibrational-rotational energy can be transferred to the Rydberg electron. This coupling between electronic and nuclear motions corresponds to a breakdown of the Born-Oppenheimer approximation. The study of the autoionizing resonances, their line profiles, and positions is of fundamental interest for the investigation of the interaction between bound states and the continuum.

The predominant coupling scheme of angular momenta in the lower lying states of many important diatomic molecules such as  $H_2$ , the alkali dimers, and NO is Hund's case (b): the orbital angular momentum  $L$  is strongly coupled to the internuclear axis with  $\Lambda$  as projection.  $\Lambda$  couples with  $N$  to  $K$  and  $K$  with  $S$  to the total angular momentum  $J$ . If an outer electron is excited to orbitals with higher main quantum numbers  $n$ , the coupling of  $L$  to the nuclear axis gets weaker and weaker. At very high  $n$  values,  $L$  is completely decoupled since the outer electron now sees an isotropic Coulomb force.

This corresponds to Hund's case (d):  $L$  and the molecular rotation vector  $N$  couple to  $J$  (spin orbit coupling is not regarded in this case). This decoupling with rising  $n$  was studied in detail in the case of  $H_2$  by Herzberg and Jungen (1972) (see also Takezawa, 1970). This work shows nicely the main features of the highly excited diatomic molecules and will be discussed here as a characteristic example.  $H_2$  has the great advantage compared with the other diatomic molecules that its rotational constant is very large, leading to clear, high-resolution absorption spectra in the ultraviolet (835 – 765 Å). The spectra of *para*- $H_2$  taken at a temperature of 80 K show that all molecules were in the lowest rotational level. Each of the vibrational levels of  $H_2^+$  was found to be the limit of two Rydberg series. At low  $n$  (Hund's case b), these are the  $np\sigma$  and  $np\pi$  series. At high  $n$  values, according to Hund's case d, the  $l$  decoupling takes place and as a result the two series converge to the appropriate  $N = 0$  and  $N = 2$  levels of the  $H_2^+$  ion and are designated as  $np0$  and  $np2$ , respectively (the *para*-character limits  $N$  to even values).

For intermediate  $n$  values there are strong perturbations between these two series. They arise from the coupling of the orbital motion of the Rydberg electron with the rotation of the  $H_2^+$  core.

In addition to these  $\Delta v = 0$  perturbations, there are also strong interactions with the vibrations of the core. They occur when a Rydberg level with  $v + 1$  is close to one with  $v$  ( $\Delta v = 1$  perturbations). After first attempts using perturbation theory (Herzberg and Jungen, 1972), the multichannel quantum defect theory (MQDT) initiated by Seaton, and elaborated by Fano, Lu, and others (see, for example, Fano, 1970, and the reviews by Seaton, 1983 and Fano, 1983) gave the complete interpretation of the very complicated spectra of  $H_2$ . This theory was also applied to discuss the more recent results on  $Na_2$  by Martin *et al.* (1983) obtained by laser spectroscopy.

The main features of MQDT for atoms have already been mentioned in Section V,C. In the following the theory will be briefly outlined with respect to molecules. In the frame of MQDT excited states, autoionization and ionization are described as scattering processes of an electron at the positive core whereby energy and angular momentum are exchanged. The above mentioned mixing of the spectral series are described in terms of channel mixing, where the channels are determined by the energy of the core, the angular momenta of core and electron, and their respective coupling.

As mentioned in Section V,C, the main idea of MQDT is that interactions between the electron and the ionic core can be separated into long- and short-range effects. When the electron is far from the core there is a Coulomb interaction and the ion – electron system is described by “collision channels”  $i$  which are analytically known. The effect of short-range non-Coulomb interaction close to and inside the core is characterized by “close coupling channels”  $\alpha$ . Effective quantum numbers  $\nu_i$  are introduced for each ioniza-

tion limit  $I_i$  of the different series ( $i = 1 \dots M$ ) by  $E = I_i - R/v_i^2$ , where  $E$  is the energy of the state and  $R$  the mass-corrected Rydberg constant. The discrete level is therefore described by a set of  $v_i$  values that satisfy the equation for the energy.

The equation

$$\det[U_{i\alpha} \sin \pi (v_i + \mu_\alpha)] = 0$$

ensures correct asymptotic behavior of the wave functions for  $r \rightarrow \infty$ ;  $\mu_\alpha$  are called the quantum defects and describe the close coupling channels  $\alpha$ , and  $U_{i\alpha}$  are the elements of an orthogonal matrix, which transform the collision channels  $i$  into the close-coupling channels  $\alpha$ .  $U_{i\alpha}$  and  $\mu_\alpha$  are treated as parameters in a fit of the above equation to the experimental data. The graphical representations of  $v_i$  versus  $v_j$  are called Lu-Fano plots.

In the case of  $H_2$ , the two channels  $np0$  and  $np2$  are taken into account, with ionization limits  $I_0, I_2$ . The effective quantum numbers are  $v_0$  and  $v_2$ . For this case, the energy equations are of the form

$$E = I_0 - 13.6 \text{ eV}/v_0^2 = I_2 - 13.6 \text{ eV}/v_2^2$$

All the discrete levels observed by Herzberg and Jungen can be fitted using this two-channel model as has been demonstrated in a Lu-Fano plot of the fitted and experimental values. In particular the  $l$  uncoupling and also the autoionization which is observed in  $H_2$  for levels above the  $N = 0$  or  $v = 0$  limit is fully accounted for (Fano, 1975; Jungen and Raoult, 1981; Dehmer et al., 1984).

## A. RYDBERG STATES OF DIATOMIC MOLECULES

### 1. $Na_2$

In the case of the  $Na_2$  molecule conventional absorption and emission spectroscopy did allow just a few lower lying states to be identified, but not Rydberg states. The investigation of the two-step labeling methods of laser spectroscopy was a prerequisite for tackling this complicated task. As will be discussed below, the application of these methods simplifies the spectra of the highly excited states. In addition the angular momenta of the states are obtained unambiguously. The optical-optical double resonance method combined with polarization spectroscopy, which gives Doppler-free lines, was successfully applied in studies of  $Na_2$ ,  $Cs_2$ , and  $Li_2$ . The principle of the experimental set-up used in these experiments is shown in Fig. 13. A polarized narrow-band laser is tuned into resonance with a known molecular transition. The laser light populates the degenerate angular momentum

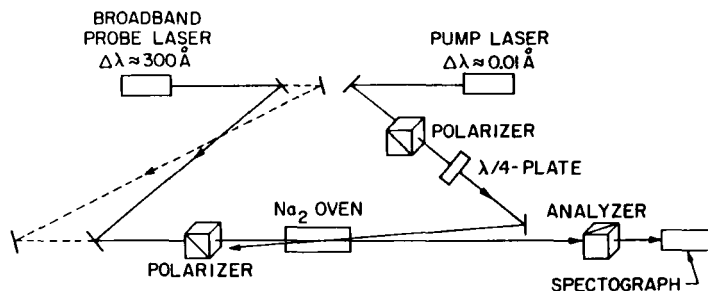


FIG. 13. Experimental arrangement of a two-step polarization labeling experiment as used by Teets *et al.* (1976) and Carlson *et al.* (1981).

sublevels of the upper state unequally, so that an orientation or alignment is obtained and, simultaneously, the sublevels of the lower state are nonuniformly depleted. This produces optical anisotropy in both levels belonging to the pumped transition. If a second linearly polarized probe laser is tuned into resonance with another molecular transition starting from one of the levels pumped with the first laser, the induced optical anisotropy causes a change in the direction of polarization of the second laser. This change can be detected using an analyzer in the second beam. The spectrum which is obtained when the second laser is tuned is greatly simplified since only transitions having a common level with the pumped transition can be observed. Highly excited states close to the ionization limit can be studied if the probe laser further excites the molecules starting from the upper level of the pumped transition. When this upper level is known, the selection rules help to determine the angular momenta of the highly excited states.

The labeling method does not require a narrow-band laser to resolve the Rydberg states as is shown in the investigation of Carlson *et al.* (1981), who used a pulsed broad-band (300-Å) probe laser. In their work 24 new electronic states with excitation energies between 28,000 and 39,000  $\text{cm}^{-1}$  were found, for which  $\Lambda$  as well as the rotational and vibrational constants were determined. The states were identified as low-lying members of Rydberg series with  $n = 3$  to 14. By extrapolation the vibrational and rotational constants of the ground state of  $\text{Na}_2^+$  are derived.

Alkali dimers such as  $\text{Na}_2$ ,  $\text{K}_2$ , and  $\text{NaK}$  in supersonic beams can be resonantly ionized by two steps via selected rovibronic intermediate states with the light of two tunable dye lasers (Herrmann *et al.*, 1978). In all these cases it was found that autoionization is important when the excitation is up to 1000  $\text{cm}^{-1}$  above the ionization threshold. In this case part of the rovibronic energy of the inner core is transferred to the outer Rydberg electron, i.e., there is strong coupling between electronic and vibrational energy resulting in a breakdown of the Born–Oppenheimer approximation.

The vibrational constants of the  $\text{Na}_2^+ 2\Sigma_g^+$  ion core were investigated in more detail by Leutwyler *et al.* (1982). They obtained good agreement with the value of Carlson *et al.* (1981), which was determined by polarization spectroscopy. The Rydberg series observed by Leutwyler *et al.* converge to five different ion core vibrational states above the ionization limit which were closely spaced. Another result of the work was an estimate of the ionization potential of  $\text{Na}_2$  which was derived from an extrapolation to  $v = 0$ .

The first assignment of very high Rydberg levels of  $\text{Na}_2$  ( $30 < n < 75$ ) was performed by Martin *et al.* (1983). The spectra were taken with a supersonic beam. The pulsed pump laser populated a well-defined intermediate rovibrational level  $v'J'$  of the  $A^1\Sigma_u^+$  or  $B^1\Pi_u$  state of  $\text{Na}_2$ . The probe laser is tuned to autoionizing Rydberg states, and so  $\text{Na}_2^+$  ions could be detected (Fig. 14). Because of the 3p character of the intermediate level, Rydberg series noted as  $ns\ ^1\Sigma_g^+$  and  $nd\ ^1\Delta_g^+$ ,  $nd\ ^1\Pi_g$  and  $nd\ ^1\Sigma_g^+$  are excited. From extrapolation to  $n \rightarrow \infty$ , the quantum defects as well as the molecular constants of  $\text{Na}_2^+$  and the

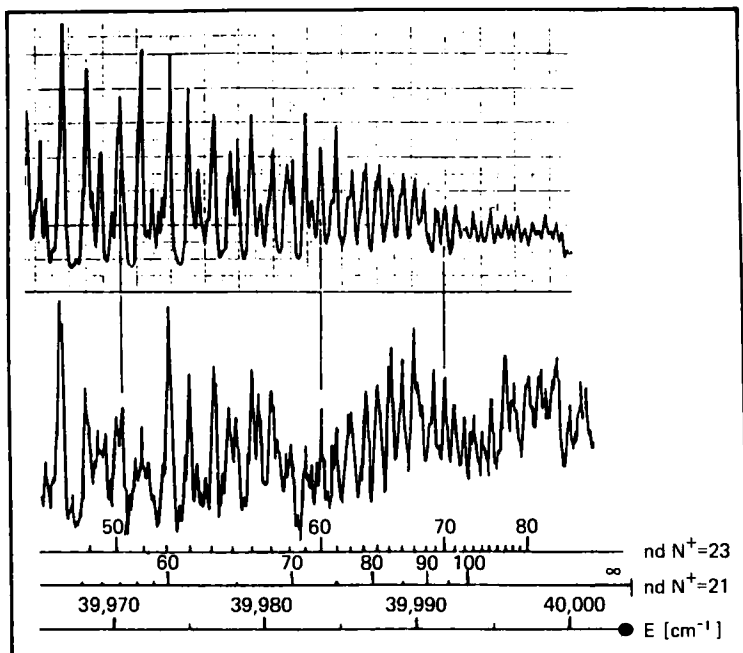


FIG. 14. Rydberg spectrum of  $\text{Na}_2$  taken by Martin *et al.* (1983) using the optical-optical double-resonance method and autoionization for detection. The signal is shown in the lower part of the figure. The lines start from the intermediate level  $v' = 4, J' = 22$  of the  $A$  state. There are two Rydberg series  $v = 4, nd\ N^+ = 21$ , and  $v = 4, nd\ N^+ = 23$  with  $n$  up to 75. This spectrum is compared with a calculated one being obtained by means of MQDT as shown in the upper part.

ionization potential of  $\text{Na}_2$  were determined. Similar to the studies in  $\text{H}_2$  the uncoupling of the angular momentum  $l$  from the internuclear axis can be observed. Then  $l$  is more strongly coupled to the rotation (Hund's case d), according to  $J = N + l$ . Also the mixing of states at lower  $n$  was observed as in  $\text{H}_2$ . Multichannel quantum defect theory was again successfully applied (Fig. 14).

## 2. $\text{Li}_2$

The experimental methods which have been used to study Rydberg states of  $\text{Na}_2$  have also been successfully applied to the spectrum of  $\text{Li}_2$ . The latter is of special interest since  $\text{Li}_2$  is the least complex stable diatomic molecule after  $\text{H}_2$ . Bernheim *et al.* (1979) began with the optical-optical double resonance labeling to investigate higher Rydberg states of  $\text{Li}_2$ . They excited  $\text{Li}_2$  in a heat pipe with two pulsed dye lasers. For the first excitation step one laser was tuned to the transition  $A^1\Sigma_u^+ \leftarrow X^1\Sigma_g^+$  and the second laser was scanned from 530–370 nm exciting gerade Rydberg states. The excitation was monitored by observing the radiation produced by collisional transfer from the gerade to ungerade states, which could then decay to the ground states by single-photon transitions.

Bernheim *et al.* (1979) identified 31 new electronic states belonging to the Rydberg series  $ns^1\Sigma_g^+$ ,  $nd^1\Sigma_g^+$ ,  $nd^1\Pi_g$  having principal quantum numbers up to  $n = 15$ . The molecular constants of the Rydberg states were determined. By extrapolating ( $n \rightarrow \infty$ ) the data of the ground state of  $\text{Li}_2^+$  were also obtained as well as the ionization potential of  $\text{Li}_2$ . *Ab initio* calculations by Konowalow and Rosenkrantz (1979) are in good agreement with these experimental results.

Extensive high-precision experiments on  $\text{Li}_2$  were performed by Demtröder *et al.* (1983). For most of the measurements the optical-optical double resonance method was used. The first laser populated the levels of the  $B^1\Pi_u$  state, the second laser is scanned through the spectral region of interest. The excited Rydberg levels decay by autoionization and the molecular ions are extracted by a small electric field and are monitored as a function of the wavelength of the second laser. The adiabatic ionization potential could be derived from the onset of the ionization continuum. Furthermore, the dissociation energy of  $\text{Li}_2^+$  was determined, being appreciably larger than that of the neutral ground state.

Because of the high complexity of the spectra resulting from perturbations when  $l$  uncouples from the figure axis with increasing  $n$ , it is also necessary to apply Doppler-free labeling methods, such as two-step polarization spectroscopy. This polarization double-resonance spectroscopy allows a distinction to be made between  $P$ ,  $Q$ , and  $R$  lines since the double resonance signals differ in sign and profile for the different transitions. The level width of upper

Rydberg levels can vary greatly, owing to predissociation, if repulsive potential curves cross the Rydberg potentials. This can be measured by Doppler-free two-photon spectroscopy.

### 3. NO

Perhaps the most complete measurements on Rydberg states of heteronuclear diatomic molecules have been performed on NO by emission and absorption spectroscopy in the vacuum ultraviolet. Most of the work was done by Miescher and co-workers (1966) and by Jungen (1970).

To study Rydberg–Rydberg transitions in NO another interesting version of the optical–optical double-resonance method is used in work by Cheung *et al.* (1983). NO gas in a cell is excited by two pulsed dye lasers, the pump laser exciting the  $A^2\Sigma^+$  level starting from the ground state. The probe laser is tuned to populated higher states. The excitation is monitored by resonance ionization of the highly excited level and by detection of the ions. The paper demonstrates, again, advantages of the methods of laser spectroscopy. Two new Rydberg transitions were analyzed and strong multistate interactions among Rydberg and valence states just below the dissociation limit were observed.

### 4. H<sub>2</sub>

Finally, Rydberg states of H<sub>2</sub> were also studied by using laser techniques. Rottke and Welge (1984) generated the 1067-Å radiation necessary to excite the intermediate state  $B^1\Sigma_u^+(v=0; J=0,1,2)$  by frequency tripling an XeCl excimer laser-pumped dye laser in a noble gas cell. A second dye laser pumped by the same excimer laser is used for the second step to reach the Rydberg states. Various Rydberg series with  $n$  up to 75 converging to different rotational states of H<sub>2</sub><sup>+</sup> were observed. The excitation of the Rydberg states was monitored for high  $n$  by field ionization and for low  $n$  by dissociation followed by one photon ionization of the product H\*. Furthermore, photoionization of H<sub>2</sub> was observed in these experiments.

## B. RYDBERG STATES OF LARGE MOLECULES

Absolute lifetimes of Rydberg states of gas phase benzene, perdeuterobenzene, toluene, and perdeuterotoluene were measured by Wiesenfeld *et al.* (1983). The Rydberg states were excited with 0.19 psec dye laser pulses. The probe beam, which was split off from the pump beam, was delayed by a

variable time and was used to ionize the excited state. The time evolution of the excited state was determined by the decay of the ion current as a function of increasing time delay. In this way absolute lifetimes from 70 to 170 fsec were measured. This is the shortest molecular process ever measured directly. The decay mechanism is unclear. However, it is probable that internal conversion to high vibrational levels of the ground state is the reason for the fast relaxation.

## IX. Rydberg Molecules

For the molecules discussed in Section VIII, Rydberg series are only observed at higher excitation energies. There exist, however, molecules for which all the transitions observed must be assigned to states showing the properties of Rydberg states, i.e., their energy is described by a Rydberg formula. The ground state of these molecules is usually dissociative. He<sub>2</sub> and ArH are well-known examples of this class of molecules, which may also be called Rydberg molecules.

More than 50 bound excited states of He<sub>2</sub> have been identified during the last 50 years. In recent years much work has been done by Ginter *et al.* (1980) to analyze and classify the spectra. In particular, they applied MQDT to analyze the triplet levels of the configuration  $(1\sigma_g)^2(1\sigma_u) n p \lambda$ ,  $n = 6-17$ . Extensive channel mixing leads here to a breakdown of conventional band models for the levels with higher  $n$ .

Metastable  $a(2s\sigma) {}^3\Sigma_u^+$  He<sub>2</sub> molecules produced in a dc discharge in a flowing He stream were excited by pulsed dye lasers by Miller *et al.* (1979). Laser-induced fluorescence spectra for the  $(np\pi) {}^3\Sigma_g^+$  series for  $n = 4-9$  and the  ${}^3\Pi_g$  series  $n = 5-15$  already known from emission spectra were observed. In addition, relaxation and fluorescence yield measurements of these states could be performed.

Spectra of excited Rydberg states of ArH and ArD were found by Johns (1970) near 7670 Å in an electric discharge through mixtures of argon and hydrogen or deuterium. So far no spectra of other rare gas monohydrides could be observed.

Also polyatomic Rydberg molecules are known, as, e.g., H<sub>3</sub>, D<sub>3</sub>, and their isotopic mixtures or NH<sub>4</sub> and ND<sub>4</sub>. These polyatomic molecules have in common that they can be thought of as being built up from their parent molecules H<sub>2</sub>, D<sub>2</sub>, NH<sub>3</sub>, and ND<sub>3</sub> by adding a proton, which is possible because of their high proton affinity. These ions are then neutralized by capturing an electron in a Rydberg orbital (Dabrowski and Herzberg, 1980).

The most extensively and successfully studied polyatomic Rydberg mole-

cules are  $H_3$  and  $D_3$ . Herzberg *et al.* (Herzberg, 1979; Herzberg *et al.*, 1980, 1981, 1982) observed their optical spectra in the light of a hollow cathode discharge through  $H_2$  and  $D_2$ , respectively. Several parallel and perpendicular electronic band systems between 5600 and 7100 Å and in the infrared near 3600 and 3950  $cm^{-1}$  were found to belong to a symmetric top molecule. The molecular constants were derived using model band calculations. In particular, the rotational constants were found to be close to those of  $H_3^+$  and  $D_3^+$ , respectively, which were predicted theoretically by Carney and Porter (1976) and measured by Oka (1980) and Shy *et al.* (1980). In this way the model of a Rydberg molecule with a triangular  $H_3^+$  core with  $D_{3h}$  symmetry and one electron in a higher orbital was established.

The bands in the visible (at 5600 and 7100 Å) were interpreted as transitions between different electronic states with the principal quantum number  $n = 3$  in the upper and  $n = 2$  in the lower state. Predissociation in the lower  $2s^2A_1'$  state leads to a line width of the lines in the two bands of 3 to 8 Å.

Owing to their large width and their high density, many lines within the bands are blends. However, the very complicated perpendicular band of  $D_3$  at 7100 Å, for example, could be resolved into single lines by a special laser labeling method (Figger *et al.*, 1983). For this purpose a line of the  $D_3$  emission spectrum of the hollow cathode discharge was selected using a monochromator. Then the beam of a dye laser is directed through the discharge and tuned. The intensity of the observed emission line changes when the laser wavelength coincides with a transition starting from the upper level of the selected transition. In this way simple spectra are obtained which are easy to assign. In particular they are free from the  $D_2$  background lines. A large amount of transitions between  $n = 3$  and  $n = 2$  could be measured by this method. With a color center laser operating in a spectral region between 2.3 and 3.3  $\mu m$ , lines have been found which seem to correspond to transitions to Rydberg states with  $n = 4$ . Such transitions could not be found spectroscopically by the conventional methods.

Before the discovery of the spectra of triatomic hydrogen, bound states with lifetimes in the microsecond region were found by neutralizing  $H_3^+$  and  $D_3^+$  ionic beams by transfer of an electron when the ions were passed through different target gases. The molecules  $H_3$  and  $D_3$  were detected by a mass spectrometer (Devienne, 1968; Nagasaki *et al.*, 1972). It is quite obvious that this production of triatomic hydrogen molecules by charge exchange is also suitable for direct observation of the spectra. For this purpose intense beams of the corresponding triatomic ions are necessary. If the source is combined with a mass selector, then the different isotopic mixtures of the triatomic hydrogen molecules can be produced and analyzed. Such experiments were recently performed by Figger *et al.* (1984) and will be described in the following.

In the apparatus a hollow cathode combined with a beam extraction system was used as ion source. The hydrogen gas pressure in the source was set at a few Torr. The acceleration voltage for the ion beam was between 4 and 20 kV. The ion beam was passed through a homogeneous magnetic field for mass selection from which beams of  $D_3^+$  and  $H_3^+$  could be separated. Beams of  $D_2H^+$  and  $H_2D^+$  could also be obtained with a suitable mixture of  $H_2$  and  $D_2$  in the hollow cathode. Typically, an extraction voltage of 12 kV yielded a  $12\text{-}\mu\text{A}$  ion beam of the selected species.

For neutralization, the ion beam was passed through an alkali vapor, which provides more effective resonant charge transfer than  $H_2$  or Ar, used in former experiments. About  $10^{-3}$  Torr of alkali vapor in a 1-cm-long cell was sufficient to neutralize about 80% of the ions. The neutralized ions appeared, at least partly, in highly excited electronic levels. They cascade to lower levels through emission of photons or simply predissociate.

Spectra of  $D_2H$ ,  $H_2D$ ,  $D_3$ , and  $H_3$  can be observed through a side window of the cell or after the neutralized molecular beam passed the cell (see Fig. 15). This experimental set-up offers a convenient method of measuring the lifetimes of single rotational states by observing the decrease of the intensity of the corresponding spectral line emitted along the beam after passing through the cell. The latter can be measured by moving the cell toward the ion source having the detector fixed in space. The procedure is similar to that in beam foil experiments.

The lifetimes are then obtained by dividing the  $1/e$  decay distance by the velocity of the molecules in the beam, which is assumed to depart little from the ion velocity before the charge exchange cell. Several of the lifetimes measured in this way for  $D_3$  agree with theoretical values calculated from electric dipole transition moments given by King and Morokuma (1979). In the cases of  $H_2D$  and  $D_2H$  the measured lifetimes are much shorter than the calculated radiative ones, showing that other decay mechanisms such as predissociation can also have an influence on the  $n = 3$  states, which does not seem to be the case for the  $D_3$  molecule.

Because of the great proton affinity of  $NH_3$  and  $ND_3$ , the ammonium radicals  $NH_4$  and  $ND_4$  are also expected to be Rydberg molecules with one outer electron orbiting around the stable  $NH_4^+$  and  $ND_4^+$  ion cores. For  $NH_4$  and  $ND_4$  two bands called Schuster and Schüler bands have been identified in the light emitted by a discharge through  $NH_3$  and  $ND_3$  (Schüler *et al.*, 1955; Schuster, 1872; Herzberg, 1981). The Schuster band was tentatively assigned to the forbidden transition  $3d\ ^2F_2 \rightarrow 3s\ ^2A_1$  (Herzberg, 1981), where  $3s\ ^2A_1$  is the ground state of the ammonium radical. The assignment of the Schüler band was discussed in the literature some time ago. Calculations of the electronic energy level system by Broclavik *et al.* (1982) and Havrilak and King (1983) suggest that it has to be assigned to the  $3p\ ^2F_2 \rightarrow 3s\ ^2A_1$

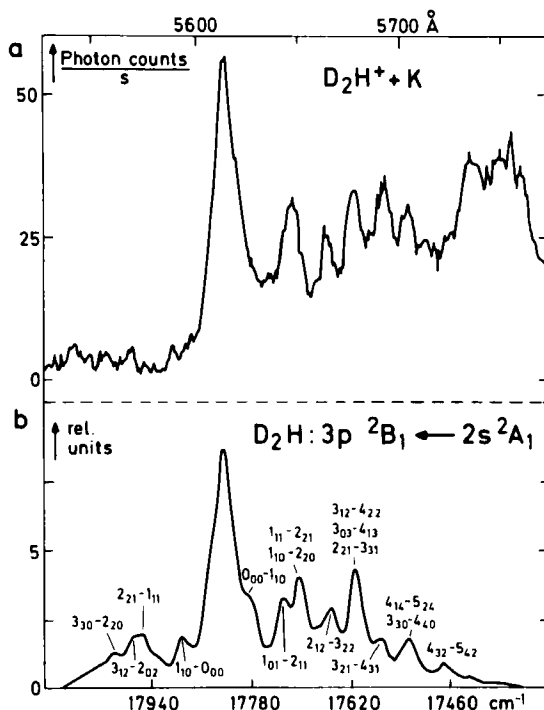


FIG. 15. (a) Emission spectrum of  $D_2H$  obtained with the beam apparatus (Figger *et al.*, 1984). (b) Computer-simulated spectrum for the  $3p \ ^2B_1 \rightarrow 2s \ ^2A_1$  band of  $D_2H$ . The numbers are asymmetric-top quantum numbers  $J_{K^-} - K^+$ . It can be seen that each peak of the experimental spectrum could be explained in the computer simulation.

transition analogously to the Na–D lines. This is also supported by two recent experiments: Gellene *et al.* (1982) found a fair degree of stability of the ground state of  $ND_4$  ( $\tau \cong 10^{-5}$  sec) in a neutralized ion beam experiment. This leads to rather clear band systems which end on the ground state, as is observed for  $ND_4$ . Whittaker *et al.* (1984) observed many lines of the Schüler band by laser frequency modulation spectroscopy. Here  $ND_4$  is formed in a photochemical reaction of  $ND_3$ . They also favor the assignment mentioned above.

#### REFERENCES

- Allen, L., and Eberly, J. H. (1975). "Optical Resonance and Two Level Atoms." Wiley, New York.  
 Aymar, M. (1984). *J. Opt. Soc. B* **1**, 239; *Phys. Rep.*, in press.

- Aymar, M., Luc-Koenig, E., and Combet-Farnoux, F. (1976). *J. Phys. B* **9**, 1279.
- Baklanov, Y. V., Chebotayev, V. P., and Dubetsky, B. Y. (1976). *Appl. Phys.* **11**, 201.
- Barbier, L., and Champeau, R.-J. (1980). *J. Phys. (Paris)* **41**, 947.
- Bates, D. R., and Damgaard, A. (1949). *Philos. Trans. R. Soc. London* **242**, 101.
- Bayfield, J. E., and Koch, P. M. (1974). *Phys. Rev. Lett.* **33**, 258.
- Beigang, R., and Timmermann, A. (1982a). *Phys. Rev. A* **25**, 1496.
- Beigang, R., and Timmermann, A. (1982b). *Phys. Rev. A* **26**, 2990.
- Beigang, R., and Timmermann, A. (1983). In "Laser Spectroscopy VI" (H. P. Weber and W. Lüthy, eds.), Vol. 40, pp. 233–236. Springer Series in Optical Sciences, Springer-Verlag, Berlin and New York.
- Beigang, R., Matthias, E., and Timmermann, A. (1981). *Phys. Rev. Lett.* **47**, 326 and erratum **48**, 290E (1982).
- Beigang, R., Matthias, E., and Timmermann, A. (1982a). *Z. Phys. A* **301**, 83.
- Beigang, R., Schmidt, D., and Timmermann, A. (1982b). *J. Phys. B* **15**, L201.
- Beigang, R., Lücke, K., and Timmermann, A. (1983). *Phys. Rev. A* **27**, 587.
- Beiting, E. J., Hildebrandt, G. F., Kellert, F. G., Foltz, G. W., Smith, K. A., Dunning, F. B., and Stebbings, R. F. (1979). *J. Chem. Phys.* **70**, 3551.
- Belfrage, C., Grafström, P., Zhan-kui, J., Jönsson, G., Levinsson, C., Lundberg, H., Svanberg, S., and Wahlström, C. G. (1983). In "Laser Spectroscopy VI" (H. P. Weber and W. Lüthy, eds.), Vol. 40, pp. 216–219. Springer Series in Optical Sciences, Springer-Verlag, Berlin and New York.
- Belin, G., Holmgren, L., Lindgren, I., and Svanberg, S. (1975). *Phys. Scr.* **12**, 287.
- Belin, G., Holmgren, L., and Svanberg, S. (1976a). *Phys. Scr.* **13**, 351.
- Belin, G., Holmgren, L., and Svanberg, S. (1976b). *Phys. Scr.* **14**, 39.
- Bethe, H. A., and Salpeter, E. E. (1957). "Quantum Mechanics of One and Two Electron Atoms." Springer-Verlag, Berlin and New York.
- Bevan, S. (1912). *Proc. R. Soc.* **86**, 320.
- Bernheim, R. A., Gold, L. P., Kelly, P. B., Kittrell, C., and Veirs, D. K. (1979). *Phys. Rev. Lett.* **43**, 123.
- Bernheim, R. A., Gold, L. P., and Tipton, T. (1983). *J. Chem. Phys.* **78**, 3635.
- Bonifacio, R., and Preparata, G. (1970). *Phys. Rev. A* **2**, 336.
- Bonifacio, R., Kim, D. M., and Scully, M. O. (1969). *Phys. Rev.* **187**, 441.
- Bonifacio, R., Schwendimann, P., and Haake, F. (1975). *Phys. Rev. A* **4**, 302.
- Broclavik, E., Mrozek, J., and Smith, V. H. (1982). *Chem. Phys.* **66**, 417.
- Brossel, I., Sagalyn, P., and Bitter, F. (1950). *Phys. Rev.* **79**, 225.
- Burgess, A. (1964). *R. Astron. Soc. Mem.* **69**, 1.
- Carlson, N. W., Taylor, A. J., Jones, K. M., and Schawlow, A. L. (1981). *Phys. Rev. A* **24**, 822.
- Carney, G. D., and Porter, R. N. (1976). *J. Chem. Phys.* **65**, 3547.
- Champeau, R. J., Leuchs, G., and Walther, H. (1978). *Z. Phys. A* **288**, 323.
- Chang, T. N. (1978). *J. Phys. B* **11**, L583.
- Chang, T. N., and Larjani, F. (1980). *J. Phys. B* **13**, 1307.
- Chang, T. N., and Poe, R. T. (1974). *Phys. Rev. A* **10**, 1981.
- Cheung, W. Y., Chupka, W. A., Colson, S. D., Gauyacq, D., Avouris, P., and Wynne, J. J. (1983). *J. Chem. Phys.* **78**, 3625.
- Cooke, W. E., and Gallagher, T. F. (1980). *Phys. Rev. A* **21**, 588.
- Cooke, W. E., Gallagher, T. F., Hill, R. M., and Edelstein, S. A. (1977a). *Phys. Rev. A* **16**, 1141.
- Cooke, W. E., Gallagher, T. F., Hill, R. M., and Edelstein, S. A. (1977b). *Phys. Rev. A* **16**, 2473.
- Curry, S. M., Collins, C. B., Mirza, M. Y., Popescu, D., and Popescu, I. (1976). *Opt. Commun.* **16**, 251.
- Dabrowski, I., and Herzberg, G. (1980). *Can. J. Phys.* **58**, 1238.

- Deech, J. S., Luypaert, R., Pendrill, L. R., and Series, G. W. (1977). *J. Phys. B* **10**, L137.
- Dehmer, P. M., Miller, P. J., and Chupka, W. A. (1984). *J. Chem. Phys.* **84**, 1030.
- Delande, D., and Gay, J.-C. (1983). *Comments At. Mol. Phys.* **13**, 275.
- Demtröder, W. (1981). "Laser Spectroscopy." Springer-Verlag, Berlin and New York.
- Demtröder, W., Eisel, D., Hemmerling, B., and Ray, B. B. (1983). In "Laser Spectroscopy VI, Proceedings of the Sixth International Conference" (H. P. Weber and W. Lüthy, eds.). Springer-Verlag, Berlin and New York.
- Devienne, M. F. (1968). *C. R. Acad. Sci. B* **267**, 1279.
- Dicke, R. H. (1954). *Phys. Rev.* **93**, 99.
- Drexhage, K. H. (1974). In "Progress in Optics (E. Wolf, ed.), Vol. 12, p. 165. North-Holland, Amsterdam.
- Eberly, J. H., Narozhny, N. B., and Sanchez-Mondragon, J. J. (1980). *Phys. Rev. Lett.* **44**, 1323.
- Edelstein, S. A., and Gallagher, T. F. (1978). *Adv. Mol. Phys.* **14**, 365.
- Eliel, E. R., and Hogervorst, W. (1983a). *J. Phys. B* **16**, 1881.
- Eliel, E. R., and Hogervorst, W. (1983b). *Phys. Rev. A* **27**, 2995.
- Eliel, E. R., Hogervorst, W., Olsson, T., and Pendrill, L. R. (1983). *Z. Phys. A* **311**, 1.
- Eriksson, K. B., and Wenåker, I. (1970). *Phys. Scr.* **1**, 21.
- Fabre, C., and Haroche, S. (1983). In "Rydberg States of Atoms and Molecules" (R. F. Stebbings and D. F. Dunning, eds.), pp. 117–164. Cambridge Univ. Press, London and New York.
- Fabre, C., Gross, M., and Haroche, S. (1975). *Opt. Commun.* **13**, 393.
- Fabre, C., Goy, P., and Haroche, S. (1977). *J. Phys. B* **10**, L183.
- Fabre, C., Haroche, S., and Goy, P. (1978). *Phys. Rev. A* **18**, 229.
- Fabre, C., Haroche, S., and Goy, P. (1980). *Phys. Rev. A* **22**, 778.
- Faist, A., Geneux, E., Meystre, P., and Quattropani, A. (1972). *Helv. Phys. Acta.* **45**, 946.
- Fano, U. (1970). *Phys. Rev. A* **2**, 353.
- Fano, U. (1975). *J. Opt. Soc. Am.* **65**, 979.
- Fano, V. (1983). *Rep. Prog. Phys.* **46**, 97.
- Farley, J. W., and Gupta, R. (1977). *Phys. Rev. A* **15**, 1952.
- Farley, J. W., and Wing, W. H. (1981). *Phys. Rev. A* **23**, 2397.
- Farley, J. W., MacAdam, K. B., and Wing, W. H. (1979). *Phys. Rev. A* **20**, 1754.
- Feneuille, S., and Jacquinet, P. (1981). *Adv. At. Mol. Phys.* **17**, 99.
- Figger, H., Leuchs, G., Straubinger, R., and Walther, H. (1980). *Opt. Commun.* **33**, 37.
- Figger, H., Moller, H., Schrepp, W., and Walther, H. (1982). *Chem. Phys. Lett.* **90**, 90.
- Figger, H., Dixit, M. N., Maier, R., Schrepp, W., Walther, H., Peterkin, I. R., Watson, J. K. G. (1984). *Phys. Rev. Lett.* **52**, 906.
- Fredriksson, K., and Svanberg, S. (1976). *J. Phys. B* **9**, 1237.
- Fredriksson, K., Lundberg, H., and Svanberg, S. (1977). *Z. Phys. A* **283**, 227.
- Fredriksson, K., Lundberg, H., and Svanberg, S. (1980). *Phys. Rev. A* **21**, 241.
- Gabrielse, G., and Dehmelt, H. (1984). To be published.
- Gabrielse, G., Van Dyck, Jr., R., Schwinberg, P., and Dehmelt, H. (1984). *Bull. Am. Phys. Soc.* **29**, 926.
- Gallagher, T. F., and Cooke, W. E. (1978). *Phys. Rev. A* **18**, 2510.
- Gallagher, T. F., and Cooke, W. E. (1979). *Phys. Rev. Lett.* **42**, 835.
- Gallagher, T. F., Hill, R. M., and Edelstein, S. A. (1976). *Phys. Rev. A* **13**, 1448, **14**, 744.
- Gallagher, T. F., Cooke, W., Edelstein, S. A., and Hill, S. (1977a). *Phys. Rev. A* **16**, 273.
- Gallagher, T. F., Humphrey, L. M., Cooke, W. E., Hill, R. M., and Edelstein, S. A. (1977b). *Phys. Rev. A* **16**, 1098.
- Gallagher, T. F., Humphrey, L. M., Hill, R. M., Cooke, W. E., and Edelstein, S. A. (1977). *Phys. Rev. A* **15**, 1937.

- Gallagher, T. F., Sandner, W., Safinya, K. A., and Cooke, W. E. (1981). *Phys. Rev. A* **23**, 2065.
- Gellene, G. I., Cleary, D. A., and Porter, R. F. (1982). *J. Chem. Phys.* **77**, 3471.
- Ginter, D. S. and Ginter, M. L. (1980) *J. Mol. Spectrosc.* **82**, 152.
- Goy, P., Fabre, C., Gross, M., and Haroche, S. (1980). *J. Phys.* **B 13**, L83.
- Goy, P., Raimond, J. M., Vitrant, G., and Haroche, S. (1982). *Phys. Rev. A* **26**, 2733.
- Goy, P., Raimond, J. M., Gross, M., and Haroche, S. (1983). *Phys. Rev. Lett.* **50**, 1903.
- Grafström, P., Zhan-Khui, J., Jönsson, G., Kröll, S., Levinson, C., Lundberg, H., and Svanberg, S. (1982). *Z. Phys. A* **306**, 281.
- Gupta, R., Chang, S., Tai, C., and Happer, W. (1972). *Phys. Rev. Lett.* **29**, 695.
- Haake, F., King, H., Schröder, G., Hans, J., and Glauber, R. J. (1979). *Phys. Rev. A* **20**, 2047.
- Haroche, S. (1971). *Ann. Phys. (Paris)* **6**, 189.
- Haroche, S. (1982). In "New Trends in Atomic Physics," Proceedings of the Summer School Session XXXVIII (G. Grynberg and R. Stera, eds.). North Holland, Amsterdam.
- Haroche, S., Fabre, C., Goy, M., Gross, M., and Raimond, J. M. (1979). In "Laser Spectroscopy IV" (H. Walther and K. W. Rothe, eds.), Vol. 21. Springer Series in Optical Sciences, Springer-Verlag, Berlin and New York.
- Haroche, S., Fabre, C., Raimond, J. M., Goy, P., Gross, M., and Moi, L. (1982). *J. Phys.* **43**, C2-265.
- Harper, C. D., and Levenson, M. D. (1976). *Phys. Lett. A* **56**, 361.
- Harvey, K. C., and Stoicheff, B. P. (1977). *Phys. Rev. Lett.* **38**, 537.
- Havriliak, S., and King, H. F. (1983). *J. Am. Chem. Soc.* **105**, 4.
- Hellmuth, T., Leuchs, G., Smith, S. J., and Walther, H. (1981). In "Lasers and Applications" (W. O. N. Guimaraes, C.-T. Lin, and A. Mooradian, eds.). Springer-Verlag, Berlin and New York.
- Herrmann, A., Leutwyler, S., Schumacher, E., and Wöste, L. (1978). *Helv. Chim. Acta* **61**, 453.
- Herzberg, G., Leutwyler, J. T., and Watson, J. K. G. (1982). *Can. J. Phys.* **60**, 1261.
- Herzberg, G. (1979). *J. Chem. Phys.* **70**, 4806.
- Herzberg, G. (1981). *Disc. Faraday Soc.* **71**, 165.
- Herzberg, G., and Jungen, Ch. (1972). *J. Mol. Spectrosc.* **41**, 425.
- Herzberg, G., and Watson, J. K. G. (1980). *Can. J. Phys.* **58**, 1250.
- Herzberg, G., Lew, H., Sloan, J. J., and Watson, J. K. G. (1981). *Can. J. Phys.* **59**, 428.
- Hogervorst, W., and Eliel, E. R. (1983). *Z. Phys. A* **310**, 19.
- Hogervorst, W., and Svanberg, S. (1975). *Phys. Scr.* **12**, 67.
- Höglund, B., and Mezger, P. G. (1965). *Science* **150**, 339.
- Hollberg, L., and Hall, J. L. (1983). In "Laser Spectroscopy VI" (H. P. Weber and W. Luthy, eds.), Vol. 40. Springer-Verlag Series in Optical Sciences, Berlin and New York.
- Holmgren, L., Lindgren, I., Morrison, J., and Martensson, A.-M. (1976). *Z. Phys. A* **276**, 179.
- Jacquinot, P., Liberman, S., and Pinard, J. (1977). *Colloq. Int. C. N. R. S.* **273**, 215.
- Jaynes, E. T., and Cummings, F. W. (1963). *Proc. IEEE* **51**, 89.
- Jeys, T. H. Foltz, G. W., Smith, K. A., Beiting, E. J., Kellert, F. G., Dunning, F. B., and Stebbings, R. F. (1980). *Phys. Rev. Lett.* **44**, 390.
- Jeys, T. H., Smith, K. A., Dunning, F. B., and Stebbings, R. F. (1981). *Phys. Rev. A* **23**, 3065.
- Johansson, I. (1961). *Ark. Fys.* **20**, 135.
- Johns, J. W. C. (1970). *J. Mol. Spectrosc.* **36**, 488.
- Jungen, Ch. (1970). *J. Chem. Phys.* **53**, 4168.
- Jungen, C. H., and Raoult, M. (1981). *Faraday Dis. Chem. Soc.* **71**, 253.
- Kaluzny, Y., Goy, P., Gross, M., Raimond, J. M., and Haroche, S. (1983). *Phys. Rev. Lett.* **51**, 1175.
- Kardashev, N. S. (1960). *Sov. Astron. (Engl. Trans.)* **3**, 813.
- Kato, Y., and Stoicheff, B. P. (1976). *J. Opt. Soc. Am.* **66**, 490.

- King, H. F., and Morokuma, K. (1979). *J. Chem. Phys.* **71**, 3213.
- Kleppner, D. (1981). *Phys. Rev. Lett.* **47**, 233.
- Kleppner, D. (1982). In "Laser-Plasma Interactions," Les Houches XXXVI, (R. Balian, ed.), pp. 733–784. North-Holland, Amsterdam.
- Kleppner, D., Littman, M. G., and Zimmerman, M. L. (1983). In "Rydberg States of Atoms and Molecules" (R. F. Stebbings and F. B. Dunning, eds.), pp. 73–116. Cambridge Univ. Press, London and New York.
- Knight, P. L., and Milonni, P. W. (1980). *Phys. Rev. C* **66**, 21.
- Knight, P., and Radmore, P. M. (1982). *Phys. Rev. A* **26**, 676.
- Knight, P., and Radmore, P. M. (1983). To be published.
- Koch, P. R., Hieronymus, H., Van Raan, A. F. J., and Raith, W. (1980). *Phys. Lett.* **75A**, 273.
- Konowalow, D. D., and Rosenkrantz, M. E. (1979). *Chem Phys. Lett.* **61**, 489.
- Kopfermann, H. (1958). "Nuclear Moments." Academic Press, New York.
- Kramers, H. A. (1923). *Phil. Mag.* **44**, 836.
- Lee, S. A., Helmcke, J., and Hall, J. L. (1978). *Opt. Lett.* **3**, 141.
- Lee, S. A., Helmcke, J., and Hall, J. L. (1979). In "Laser Spectroscopy IV" (H. Walther and K. W. Rothe, eds.), Vol. 21. Springer-Verlag Series in Optical Sciences, Berlin and New York.
- Leuchs, G. (1983). In "Laser Physics" (J. D. Harvey and D. F. Walls, eds.), Vol. 182. Lecture Notes in Physics, Springer-Verlag, Berlin and New York.
- Leuchs, G., and Walther, H. (1977). In "Laser Spectroscopy III" (J. L. Hall and J. L. Carlsten, eds.) Springer-Verlag, Berlin and New York.
- Leuchs, G., and Walther, H. (1979). *Z. Phys. A* **293**, 93.
- Leuchs, G., Smith, S. J., Khawaja, E. E., and Walther, H. (1979). *Opt. Commun.* **31**, 313.
- Leutwyler, S., Heinis, T., and Jungen, M. (1982). *J. Chem. Phys.* **76**, 4290.
- Liao, P. F., Freeman, R. R., Panock, R., and Humphrey, L. M. (1980). *Opt. Commun.* **34**, 195.
- Lieberman, S., and Pinard, J. (1979). *Phys. Rev. A* **20**, 507.
- Lindgren, I., and Martensson, A.-M. (1982). *Phys. Rev. A* **26**, 3249.
- Lindgren, I., and Morrison, J. (1982). "Atomic Many-body Theory." Springer Series in Chemical Physics 13, Springer-Verlag, Berlin and New York.
- Lindgren, I., and Rosen A. (1974). *Case Stud. At. Phys.* **4**, 97.
- Lindgren, I., Lindgren, J., and Martensson, A.-M. (1976a). *Z. Phys. A* **279**, 113.
- Lindgren, I., Lindgren, J., and Martensson, A.-M. (1976b). *Phys. Rev. A* **13**, 165.
- Littman, M. G., Kash, M. M., and Kleppner, D. (1978). *Phys. Rev. Lett.* **41**, 103.
- Livering, G. D., and Dewar, J. (1879). *Proc. R. Soc. London* **29**, 398.
- Lorenzen, C. J., and Niemax, K. (1979). *J. Quant. Spectrosc. Radiat. Transfer* **22**, 247.
- Lorenzen, C. J., Weber, K.-H., and Niemax, K. (1980). *Opt. Commun.* **33**, 271.
- Lorenzen, C. J., Niemax, K., and Pendrill, L. R. (1981). *Opt. Commun.* **39**, 370.
- Lu, K. T., and Fano, U. (1970). *Phys. Rev. A* **2**, 81.
- Luc-Koenig, E. (1976). *Phys. Rev. A* **13**, 2114.
- Luk, T. S., DiMauro, L., Feldman, M., and Metcalf, H. (1981). *Phys. Rev. A* **24**, 864.
- McGillivray, J. C., and Feld, M. S. (1976). *Phys. Rev. A* **14**, 1169; *Phys. Rev.* **A23**, 1334.
- Martin, S., Chevalleyre, J., Bordas, M. Chr., Valignat, S., Broyer, M., Caboud, B., and Hoareau, A. (1983). In "Laser Spectroscopy VI, Proceedings of the Sixth International Conference" (H. P. Weber and W. Lüthy, eds.). Springer-Verlag, Berlin and New York.
- Menzel, D. H., and Pekeris, C. L. (1935). *Monthly Notices R. Astron. Soc.* **96**, 77.
- Meschede, D. (1984). Ph.D. thesis, University of Munich.
- Meschede, D., and Walther, H. (1983). Unpublished material.
- Meschede, D., and Walther, H. (1984) to be published.
- Meystre, P., Geneux, E., Quattropiani, A., and Faist, A., (1975). *Nuovo Cim. B* **25**, 521.

- Miescher, E. (1966). *J. Mol. Spectrosc.* **20**, 130.
- Miller, T. A., and Bondbey, V. E. (1979). *J. Mol. Spectrosc.* **78**, 120.
- Milonni, P. W., and Knight, P. L. (1973). *Opt. Commun.* **9**, 119.
- Mingguang, L., Yinde, W., Chongye, W., Li, L., Fangyong, S., Shying, Y., Shangjun, H., Zengliang, C., Junxiang, L., Ze, F., Yi, Z., and Qingshi, Z. (1982). *Laser J. (China)* **9**, 434. [*Phys. Abstr.* **96**, 1712 (1983). Abstr. 21692].
- Moi, L., Fabre, C., Goy, P., Gross, M., Haroche, S., Encrenaz, P., Beaudin, G., and Lazareff, B. (1980). *Opt. Commun.* **33**, 47.
- Moi, L., Goy, P., Gross, M., Raimond, J. M., Fabre, C., and Haroche, S. (1983). *Phys. Rev. A* **27**, 2043, 2065.
- Moore, Ch. (1971). "Atomic Energy Levels," National Bureau of Standards NSRDS-NBS-35 Vol. I-III, Washington, D.C.
- Nagasaki, T., Doi, H., Wada, K., Higashi, K., and Fukuzawa, F. (1972). *Phys. Lett. A* **38**, 381.
- Nakayama, S., Kelly, F. M., and Series, G. W. (1981). *J. Phys. B* **14**, 835.
- Neijzen, J. H. M., and Dönszelman, A. (1982). *J. Phys. B* **15**, 1981.
- Neukammer, J., and Rinneberg, H. (1982a). *J. Phys. B* **15**, L425.
- Neukammer, J., and Rinneberg, H. (1982b). *J. Phys. B* **15**, 2899.
- Neukammer, J., and Rinneberg, H. (1982c). *J. Phys. B* **15**, L723.
- Niemax, K., and Pendrill, L. (1980). *J. Phys. B* **13**, L461.
- Nillsson, L., and Svanberg, S. (1979). *Z. Phys. A* **291**, 303.
- Oka, T. (1980). *Phys. Rev. Lett.* **45**, 531.
- Pendrill, L. R. (1983). *Physica Scripta* **27**, 371.
- Polder, D., Schuurmans, M. F. H., and Vrehen, Q. H. F. (1979). *Phys. Rev. A* **19**, 1192.
- Popescu, I., Ghita, C., Popescu, D., and Musa, G. (1966). *Ann. Phys. (Leipzig)* **18**, 103.
- Purcell, E. M. (1946). *Phys. Rev.* **69**, 681.
- Pyper, N. C., and Marketos, P. (1981). *J. Phys. B* **14**, 4469.
- Raimond, J. M., Goy, P., Gross, M., Fabre, C., and Haroche, S. (1982a). *Phys. Rev. Lett.* **49**, 117.
- Raimond, J. M., Goy, P., Gross, M., Fabre, C., and Haroche, S. (1982b). *Phys. Rev. Lett.* **49**, 1924.
- Raimond, J. M., Goy, P., Gross, M., Fabre, C., and Haroche, S. (1983). In "Laser Spectroscopy VI" (H. P. Weber and W. Lüthy, eds.), Vol. 40, pp. 237-241. Springer Series in Optical Sciences, Springer-Verlag, Berlin and New York.
- Rausch von Traubenberg, H., Gebauer, R., and Lewin, G. (1930). *Naturwissenschaften* **18**, 417.
- Rempe, G. (1981). Diploma Thesis, University of Munich.
- Rinneberg, W. (1984). In "Progress in Atomic Spectroscopy" (H. Kleinpoppen and H. J. Beyer, eds.), Vol. D. Plenum, New York, in press.
- Rinneberg, W., and Neukammer, J. (1982a). *J. Phys. B* **15**, L825.
- Rinneberg, W., and Neukammer, J. (1982b). *Phys. Rev. Lett.* **49**, 124.
- Rinneberg, W., and Neukammer, J. (1983). *Phys. Rev. A* **27**, 1979.
- Rinneberg, W., Neukammer, J., Majewski, V., and Schonhense, G. (1983). *Phys. Rev. Lett.* **51**, 1546.
- Risberg, P. (1956). *Ark. Fys.* **10**, 583.
- Rottke, H., and Welge, K. (1984). "Proceedings of the Colloque International du CNRS on Atomic Collisions in a Laser Field, Abbaye de Royaumont, France," in press.
- Rubbmark, J. R., Kash, M. M., Littman, M. G., and Kleppner D. (1981). *Phys. Rev. A* **23**, 3107.
- Rydberg, J. R. (1889). *Kgl. Sven. Vedensk. Akad. Handl.* **23**, Sections 15 and 16.
- Scharf, G. (1970). *Helv. Phys. Acta* **43**, 806.
- Schüler, H., Michel, A., and Grün, A. E. (1955). *Z. Naturforsch.*, **10a**, 1.
- Schuster, A. (1872). *Rep. Br. Assoc.* **38**.

- Seaton, M. J. (1966). *Proc. Phys. Soc. (London)* **88**, 801.
- Seaton, M. J. (1983). *Rep. Prog. Phys.* **46**, 167.
- Shy, J. T., Farley, J. W., Lamb, W. E., and Wing, W. H. (1980). *Phys. Rev. Lett.* **45**, 535.
- Solarz, R. W., May, C. A., Carlson, L. R., Worden, E. F., Johnson, S. A., and Paisner, J. A. (1976). *Phys. Rev. A* **14**, 1129.
- Stebbing, R. F., (1979). *Adv. At. Mol. Phys.* **15**, 77.
- Stebbing, R. F., Latimer, C. J., West, W. P., Dunning, F. B., and Look, T. B. (1975). *Phys. Rev. A* **12**, 1453.
- Sternheimer, R. M., Rodgers, J. E., and Das, T. P. (1978). *Phys. Rev. A* **17**, 505.
- Stoicheff, B. P., and Weinberger, E. (1979). *Can. J. Phys.* **57**, 2143.
- Svanberg, S. (1977). In "Laser Spectroscopy III" (J. L. Hall and J. L. Carlsten, eds.), Vol. 12, pp. 183–194. Springer-Verlag Series in Optical Sciences, Berlin and New York.
- Takezawa, S. (1970). *J. Chem. Phys.* **52**, 5793.
- Teets, R., Feinberg, R., Hänsch, T. W., and Schawlow, A. G. (1976). *Phys. Rev. Lett.* **37**, 683.
- Townes, C. H., and Schawlow, A. G. (1955). "Microwave Spectroscopy." McGraw-Hill, New York.
- Vaidyanathan, A., Spencer, W., and Kleppner, D. (1981). *Phys. Rev. Lett.* **47**, 1592.
- Vasilenko, L. S., Chebotayev, V. P., and Shishayer, A. V. (1970). *JETP Lett.* **12**, 161.
- Vialle, J. L., and Duong, H. T. (1979). *J. Phys. B* **12**, 1407.
- Wangler, J. Henke, J., Wittmann, W., Plöhn, H. J., and Andrä, H. J. (1981). *Z. Phys. A* **299**, 23.
- Wiesenfeld, J. M., and Greene, B. I. (1983). *Phys. Rev. Lett.* **51**, 1745.
- Whittaker, E. A., Sullivan, B. J., Bjorklund, G. C., Wendt, H. R., and Hunziker, H. E. (1983). *J. Chem. Phys.* **80**, 961.
- Wittke, J. P. (1975). *RCA Rev.* **36**, 655.
- Wood, R. W. (1916). *Astrophys. J.* **43**, 73.
- Zhan-kui, J., Lundberg, H., and Svanberg, S. (1982). *Z. Phys. A* **306**, 7.